Am J Cancer Res 2024;14(5):2371-2389
www.ajcr.us /ISSN:2156-6976/ajcr0156662

Original Article

LINC00908 attenuates LUAD tumorigenesis through DEAD-box helicase 54

Jiahua Zhao[1*], Xuhui Yang[2*], Wenwen Gong[3*], Lin Zhang[4*], Chenxi Li[2], Xiao Han[2], Yang Zhang[5], Xiangyang Chu[6]

[1]Department of Thoracic Surgery, The Sixth Medical Center, Chinese PLA General Hospital and Chinese PLA Medical School, Beijing, China; [2]Department of Oncology, The Fifth Medical Center, Chinese PLA General Hospital and Chinese PLA Medical School, Beijing, China; [3]Department of Pharmacy, The Medical Supplies Center of PLA General Hospital, Beijing, China; [4]Department of Outpatient Service, 986th Hospital Affilliated to Air Force Medical University, Xi'an, Shaanxi, China; [5]Department of Cardiology, The Second Medical Center, Chinese PLA General Hospital, Beijing, China; [6]Department of Thoracic Surgery, The First Medical Center, Chinese PLA General Hospital and Chinese PLA Medical School, Beijing, China. [*]Equal contributors.

Received March 19, 2024; Accepted May 6, 2024; Epub May 15, 2024; Published May 30, 2024

Abstract: Lung adenocarcinoma (LUAD) is one of the leading causes of cancer-related death worldwide. We identified a specific long non-coding RNA (LncRNA), LINC00908, which was downregulated in LUAD tissues and associated with good outcome. LINC00908 inhibited glycolysis by regulating the expression of the DEAD-box helicase 54 (DDX54), which was screened by a nine-gene risk signature, where DDX54 showed a positive correlation with several glycolysis-related genes. Experimental verification confirmed that DDX54 regulated nine key glycolytic enzymes, thereby affecting the level of glycolysis in LUAD. Further, the expression of LINC00908 in LUAD tumorigenesis was modulated by a transcription factor, regulatory factor X2 (RFX2). The RFX2/LINC00908/DDX54 axis regulated LUAD tumor growth, migration, invasion, cell apoptosis and glycolysis both *in vitro* and *in vivo*. These results demonstrate that this axis may serve as a novel mediator in LUAD progress and offer a novel therapeutic target for more precise diagnosis and treatment of LUAD.

Keywords: Lung adenocarcinoma, LINC00908, DDX54, RFX2, glycolysis

Introduction

Lung cancer is the leading reason of tumor-associated death worldwide, with the incidence rising by approximately 4.5% annually [1, 2]. LUAD, a primary histological type of lung cancer, has seen significant advancements in targeted therapy and oncogene discovery in recent decades [3]. However, a large proportion of LUAD still lack effective targeted therapy options.

Reprogramming the energy metabolism is characterized by the "Warburg effect", one of the most important emerging markers of cancer [4, 5]. It is widely characterized that high levels of glycolysis occur regardless of the existence of oxygen, facilitating increased glucose uptake, lactic acid production and ATP production, which in turn promote tumor growth and progressions [6]. Therefore, glycolysis is a complex, multi-step and long-term process in the development of most cancer types, including LUAD [7].

Over the past decades, the essential role of noncoding RNAs (ncRNAs) in the regulation of gene expression has been widely recognized, including the phenotype of normal or tumor cells [8]. Long non-coding RNAs (LncRNAs), defined as genomic transcripts with a length of more than 200 nucleotides, do not encode proteins due to the absence of a sufficient open reading frame. However, plenty of existing studies have confirmed that LncRNAs are involved in the oncogenesis and progression of tumors, serving as effective cancer biomarkers and potential therapeutic targets [9]. LncRNAs are found to have profound impacts on diverse downstream targets, acting as competitive

endogenous RNAs (ceRNAs) to upregulate mRNAs expression through adsorbing microRNAs. For example, LINC-PINT regulates miR-767-5p biogenesis in thyroid cancer [10]. Besides, LncRNAs can regulate tumor oncogenesis by binding to RNA binding protein (RBP) to maintain mRNA stability. For instance, LncRNA LBX2 antisense RNA 1 positively regulates LBX2 mRNA stability via Fused in sarcoma [11].

DDX proteins, the largest subfamily of RNA helicase SF2, unfold RNA double strand and participate in multiple processes of RNA metabolism, including RNA cutting, editing, output and degradation, as well as the conduct of ribosome generation, transcription and translation [12]. At present, more than 50 DDX family members have been identified and studied in relation to cancer, such as DDX3 and DDX5 [13-15]. Therefore, DDX memberships might be potential targets for tumor diagnosis, prognosis evaluation and drug treatment. DDX54 has been proved to be a hormone-dependent interacting protein of estrogen receptors (ERs) and CAR-binding protein [16, 17]. In addition, DDX54 involves in DNA damage repair, promoting the growth of gastric cancer cells and the formation of myelin sheath of nerve cells [18]. However, the precise function and mechanisms of DDX54 in LUAD have not been established.

In our study, LINC00908 was first proved to be negatively correlated with DDX54, and it predicted a good clinical prognosis in LUAD. Mechanistically, LINC00908 inhibits the expression of glycolysis related genes by downregulating the expression of DDX54. In addition, the expression of LINC00908 is mainly activated by the transcription factor, RFX2. The results show that RFX2/LINC00908/DDX54 axis regulates glycolysis, tumor growth and lung metastasis of LUAD in vitro and in vivo. Our study established RFX2/LINC00908/DDX54 as a new key axis to regulate the growth and progress of LUAD.

Materials and methods

Human tumor tissues and cell lines

Normal lung cell line (16HBE) and LUAD cell lines (A549, PG49, H1299, Calu3) used in this study were all incubated in Dulbecco's Modified Eagle Medium (GIBCO, USA) blended with fetal bovine serum (10%), penicillin (100 IU/mL) and streptomycin (100 mg/mL) at 37°C with 5% CO_2.

130 LUAD samples were acquired from patients who underwent surgery from March to September 2019 at Chinese PLA General Hospital. The Ethics Committee of Chinese PLA General Hospital supervised all experimental processes.

Analysis of TCGA-LUAD dataset

The Cancer Genome Atlas (TCGA) database (https://portal.gdc.cancer.gov/repository) provided the RNA-Sequencing and corresponding clinical information for the analysis. Differentially expressed lncRNAs/mRNAs ($|log2FC| > 1$ and P-value < 0.05) were identified using limma package in R. The correlation between different lncRNAs/mRNAs was analyzed by the Spearman algorithm. KMplotter tool was employed to explore lncRNA or mRNA related to the prognosis of LUAD patients. The gene enrichment analysis (GSEA) was conducted to find possible mechanism of tumorigenesis in LUAD.

qRT-PCR

RNA was obtained from human tumor tissues or cells by using Trizol reagent following the manufacturer's instructions. The obtained RNA was then transcribed into cDNA using qPCR. The comparative Ct value (ΔCt) was used to determine the relative expression levels of genes. Specific primer sequences are listed in Supplementary Table 1.

Western blot

Cells and tissues were lysed in RIPA lysis buffer, and the extracted proteins were separated on SDS-PAGE gels, which were further transferred to the polyvinylidene fluoride (PVDF) membrane. The primary antibodies and secondary antibodies were then employed sequentially. The primary antibodies included anti-DDX54 (26894-1-AP, Proteintech; 1:1,000 dilution), anti-RFX2 (ab79241, Abcam; 1:500 dilution), anti-β-actin (sc-47778, Santa Cruz Biotechnology; 1:1,000 dilution), anti-SLC2A1 (21829-1-AP, Proteintech; 1:500 dilution), anti-HK2 (2867S, Cell Signaling Technology; 1:500 dilution), anti-GPI (sc-33777, Santa Cruz Biotechnology; 1:500 dilution), anti-PFKL (sc-

292523, Santa Cruz Biotechnology; 1:500 dilution), anti-ALDOA (11217-1-AP, Proteintech; 1:1,000 dilution), anti-GAPDH (G9295, Sigma-Aldrich; 1:1,000 dilution), anti-PGK1 (17811-1-AP, Proteintech; 1:1,000 dilution), anti-PGAM1 (16126-1-AP, Proteintech; 1:1,000 dilution), anti-ENO1 (sc-15343, Santa Cruz Biotechnology; 1:500 dilution), anti-PKM (sc-365684, Santa Cruz Biotechnology; 1:500 dilution), anti-LDHA (19987-1-AP, Proteintech; 1:1,000 dilution).

Cell proliferation, colony-formation, and apoptosis assays

CCK-8 was used to detect the proliferation ability of cells following the instructions. Cells (3×10^3/well) were cultured in a 3.5 cm plate for 2 weeks. After being rinsed twice with PBS, the cells were fixed with 4% formaldehyde for 30 minutes. Afterwards, the cells were rinsed twice with PBS again and stained with 0.1% crystal violet solution for 30 min. Colonies larger than 1.5 mm in diameter were counted. Apoptosis rates were determined by dissociating cells and staining with an Annexin V Apoptosis Detection Kit, followed by flow cytometry analysis.

Cell migration and invasion assays

For the migration assay, cells were plated, and a straight line was drawn across the cells with 200 μL pipette tips. Cells were cultured for 24 h, after which the wound edges were photographed and calculated. For the invasion assay, cell invasion chambers were applied as the manufacturer's protocol. The cells were seeded into the upper chamber with serum-free medium. After 24 h, 4% paraformaldehyde was used to fix cells adhering on the surface of the lower chambers. Following the rinse with PBS twice, the cells were stained with 0.5% crystal violet and photographed with a microscope.

Extracellular acidification rate (ECAR) and oxygen consumption rate (OCR)

The Seahorse XFe96 Extracellular Flux Analyzer was used to detect ECAR and OCR as the manufacturer's protocols. The indicated cells were resuspended and counted. 10,000 cells were transferred into Seahorse XF96 cell culture microtiter plate. Both for ECAR or OCR detection, the baselines were detected first. Glucose, oligomycin and 2-deoxyglucose were sequentially added in proper time for ECAR detection. Oligomycin, FCCP, and a mixture of rotenone and antimycin A (Rote/AA) were added in proper time and order for OCR. ECAR values were shown as mpH/min, and OCR values were shown as pmols/min.

Chromatin immunoprecipitation (ChIP) assay

For ChIP assays, cells were fixed with formaldehyde to form DNA-protein mixture for 10 min. The fixation reaction was stopped by the addition of glycine. The cell lysates were subjected to sonication treatment and immunoprecipitated with specific antibodies. DNA was extracted and purified from the immunoprecipitated complex and analyzed by PCR.

Luciferase reporter assay

The promoter of LINC00908 and its various segments were cloned into pGL3.0-basic vector respectively. Cells were co-transfected with luciferase reporters, and the luciferase activities were measured after 24 h according to the manufacturer's protocol.

Hematoxylin-eosin and IHC assay

Paraffin-embedded tissues were sectioned into 4 mm thickness. Following antigen retrieval, sections were incubated with specific primary antibodies, washed, then incubated with corresponding secondary antibodies. Visualization was achieved through application of 3,3-diaminobenzidine (DAB) and counterstaining with hematoxylin.

Tumor growth and metastasis analysis in vivo

To assess cell proliferation *in vivo*, mice (n = 7 per group) were injected in the axillary fossae with 1 × 10^7 A549 cells carrying different constructs. Overall survival and tumor size were evaluated at the indicated times. The mice were euthanized by rapid cervical dislocation to obtain tumor tissue. The time of sacrifice was recorded. The Ethics Committee of Chinese PLA General Hospital supervised all of the animal experiments.

Statistical analysis

All experiments were repeated at least three times, and the data were shown as averages

from these repeated experiments. GraphPad 8.0 and SPSS 22.0 were used for statistical analysis of all experimental data. The difference between two groups was analyzed by two-tailed Student's test, and the differences among multiple groups were tested by ANOVA. A *p* value of less than 0.05 was considered statistically significant.

Results

Screening of LncRNAs and characterization of LINC00908 in LUAD

To identify new effective LncRNAs regulating glycolysis in LUAD, we analyzed the data related to LUAD according to the screening strategy (**Figure 1A**). The differentially expressed LncRNAs in normal and cancer tissues were identified using data from TCGA database. As shown in **Figure 1B**, there were 1843 differentially expressed LncRNAs, including 992 upregulated and 851 downregulated LncRNAs in paired samples. In addition, 1906 differentially expressed LncRNAs were screened in unpaired samples involving 883 upregulated and 1023 downregulated LncRNAs (Supplementary Figure 1). Overall, there were 1491 overlapped LncRNAs comprising 790 upregulated and 701 downregulated LncRNAs (**Figure 1C**).

Next, we analyzed these differentially expressed LncRNAs in relation to survival by independent prognostic analysis. The overall prognosis was correlated with 8 upregulated LncRNAs, including LINC00908, and 5 downregulated LncRNAs (**Figure 1D**). Subsequently, we explored the correlation between the prognosis-associated LncRNAs and a nine-gene risk score associated with glycolysis. Interestingly, LINC00908 had the greatest correlation coefficient with risk score among these 13 LncRNAs (**Figure 1E**), indicating its possible role in LUAD. Moreover, the expression of LINC00908 in normal tissues was higher than that in tumor tissues (**Figure 1F**, **1G**). Further analysis found that LINC00908 was positively associated with good clinical outcome in LUAD (**Figure 1H**). Additionally, we analyzed LUAD RNA-seq data for gene set enrichment analysis (GSEA). Consistently, LINC00908 was negatively correlated with poor survival of lung cancer (**Figure 1I**). To further explore specific functions of LINC00908 in LUAD, RNA levels were determined in 10 pairs of LUAD tissues and their matched adjacent normal tissues by qRT-PCR. The results similarly demonstrated that LINC00908 expressions in cancer tissues were significantly lower than that in normal tissues (**Figure 1J**). Notably, LINC00908 expressions in tumor cells were lower than that in normal lung epithelial cells, remarkably lower in A549 and H1299 cells (**Figure 1K**).

DDX54, a negative prognostic factor for LUAD, was regulated by LINC00908

The mechanisms by which LINC00908 regulates glycolysis in LUAD were further explored. First, LUAD patients in TCGA database were divided into high and low risk score sets employing the above-mentioned nine-gene risk signature model. Our analysis identified 1 upregulated and 1837 downregulated differential expressed genes in our screen (**Figure 2A**). Subsequently, 25 target genes potentially regulated by LINC00908 were predicted based on the Starbase database. By intersecting the 25 target genes and 1838 differentially expressed genes, we obtained 3 potential genes, DDX54, IGF2BP3 and TAF15, likely influenced by LINC00908 (**Figure 2B**). Excitingly, the highest correlation was observed between DDX54 and LINC00908 (**Figure 2C**, Supplementary Figure 2). We thus gave priority to the possible regulatory relationship between LINC00908 and DDX54. In 10 paired LUAD and adjacent tissues, mRNA and protein levels of DDX54 were significantly higher in LUAD tissues (**Figure 2D**). This finding was consistent with analyses of both paired and unpaired data from the TCGA database (**Figure 2E**). Furthermore, high DDX54 expression levels resulted in a poor OS in LUAD (**Figure 2F**). In addition, the pivotal results were that knockdown of LINC00908 significantly fueled DDX54 expressions both in A549 and H1299 cells (**Figure 2G**). In total, the intrinsic mechanisms of DDX54 and LINC00908 in LUAD deserve to be estimated.

LINC00908/DDX54 regulated proliferation, migration, invasion and apoptosis in LUAD cells

Next, we detected the roles of LINC00908 and DDX54 in the growth, apoptosis, migration and invasion in various LUAD cells. LINC00908 overexpression decreased the protein levels of DDX54 in both A549 and H1299 cells. Remarkably, this impairing effect can be reversed by DDX54 overexpression in the cells transfected with LINC00908 (**Figure 3A**,

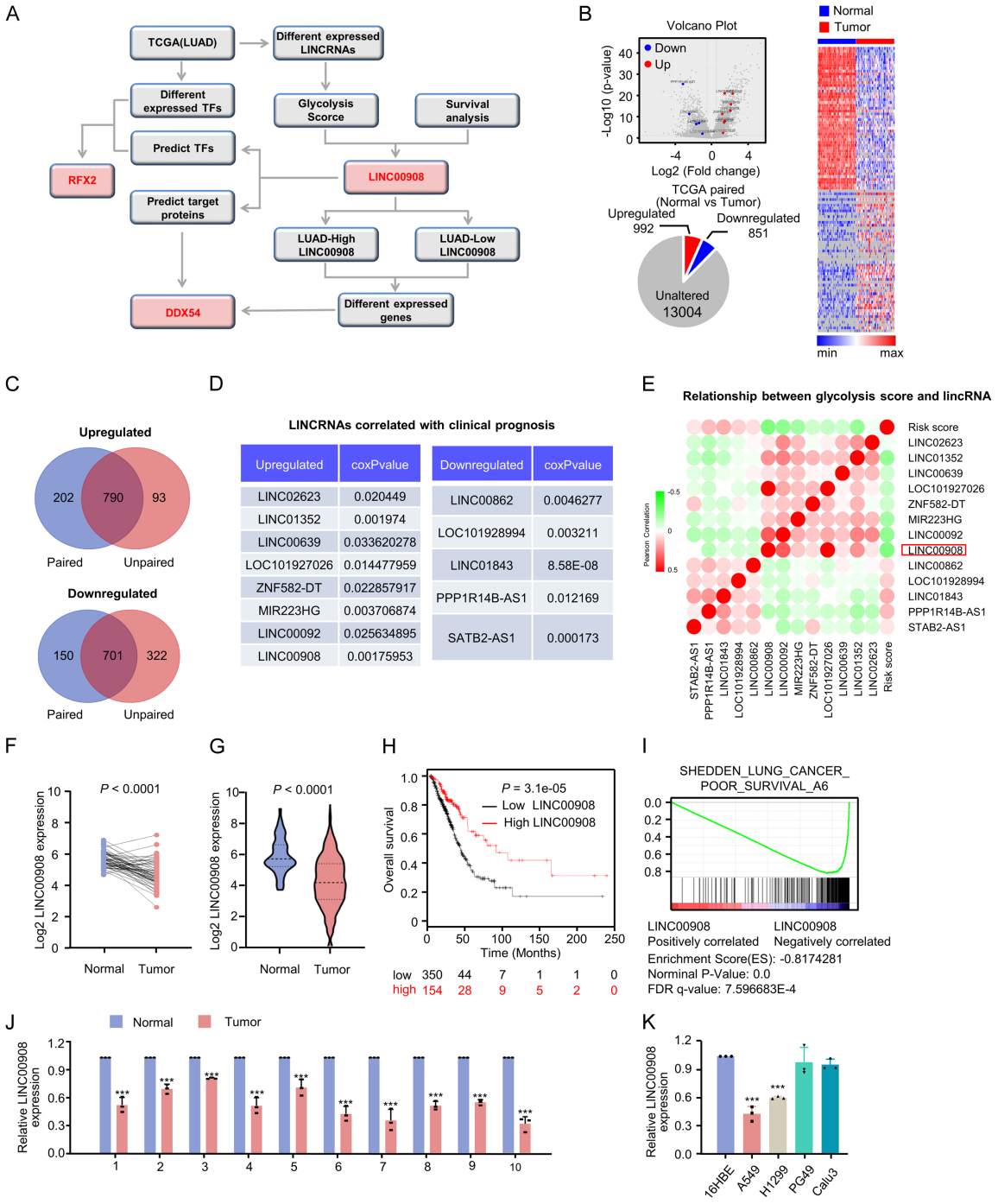

Figure 1. Screening of LncRNAs and characterization of LINC00908 in LUAD. A. Screening flowchart. B. A volcano plot illustrating differential LncRNA expressions between paired normal and tumor LUAD tissues based on TCGA database. Values are presented as the $\log_{10}$ of tag counts. C. Venn analysis of the differentially regulated LncRNAs. The overlapped portion represents the intersection of differentially regulated LncRNAs in paired and unpaired LUAD tissues. D. Screened LncRNAs in the TCGA clinical database by independent prognostic analysis. E. Correlations between clinical prognosis-related LncRNAs and the risk score related to glycolysis. F and G. LINC00908 expressions in TCGA LUAD database. H. Kaplan-Meier estimate of overall survival related to LINC00908 expressions in LUAD patients. I. GSEA plot for LINC00908 expression in the TCGA LUAD dataset. J. RT-PCR analysis of LINC00908 expressions in 10 paired adjacent and tumor tissues. K. Expression of LINC00908 in one human bronchial epithelioid cell and four LUAD cell lines by RT-PCR. ***P < 0.0001.

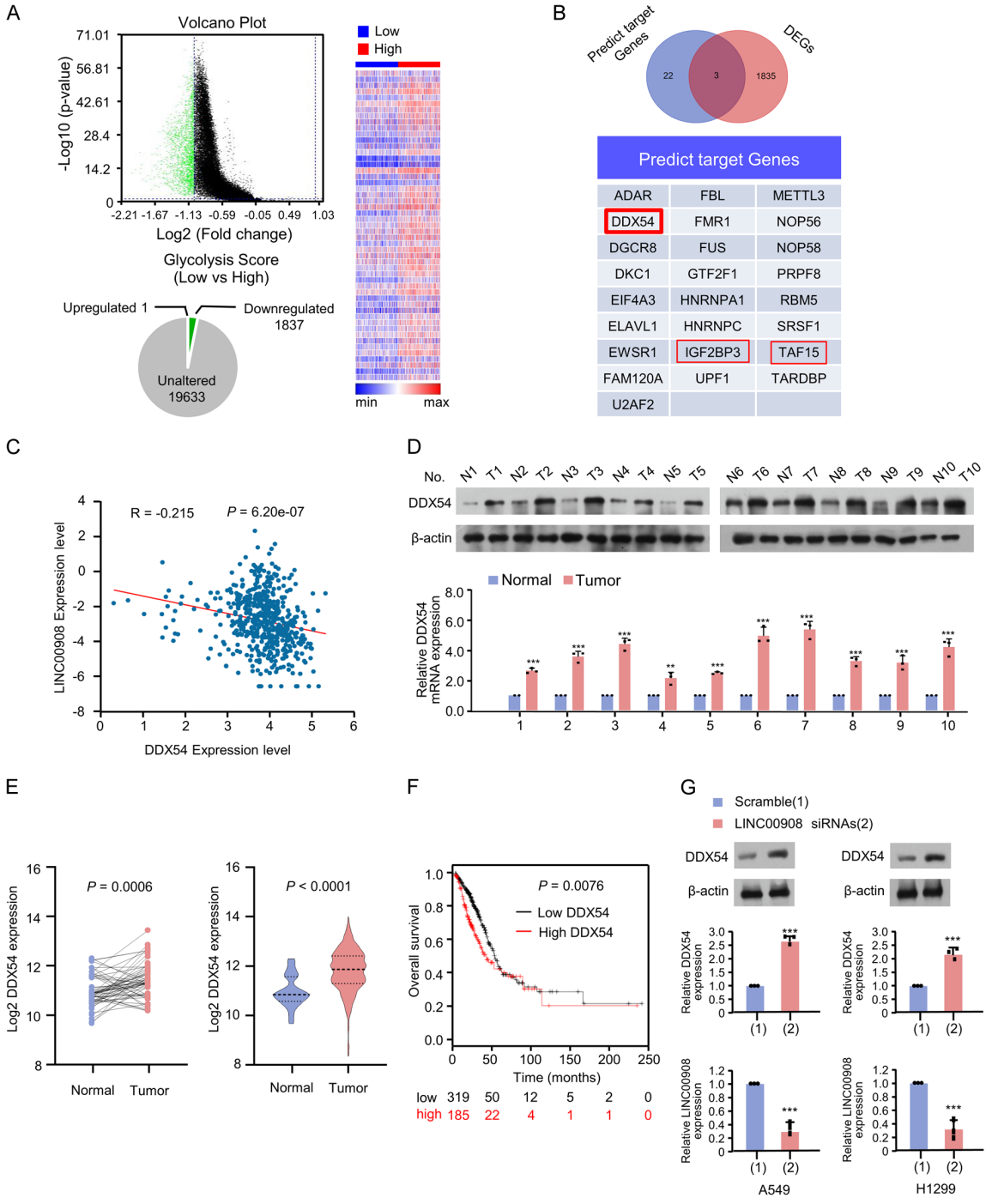

Figure 2. DDX54, a negative prognostic factor for LUAD, is regulated by LINC00908. A. Volcano plot illustrating differentially expressed genes (DEGs) from RNA-seq analysis between high and low risk score. Values are presented as the log10 of tag counts. Pie chart showed screened genes. The hierarchical clustering of the RNA-seq analysis for differently expressed genes. B. Venn diagram of target genes of LINC00908 (bottom table) by https://starbase.sysu.edu.cn (left) or DEGs (right). C. The relationship between the expression of LINC00908 and DDX54 in LUAD based on TCGA database by online analysis (https://starbase.sysu.edu.cn). D. DDX54 expression in 10 paired tumor and adjacent normal tissues. E. DDX54 expression in tumor and adjacent normal tissues in TCGA database. F. Kaplan-Meier estimate of overall survival (OS) for LUAD patients from TCGA (http://kmplot.com/analysis/). G. The DDX54 mRNA and protein levels and LINC00908 mRNA levels in LUAD cell lines. ***P < 0.0001.

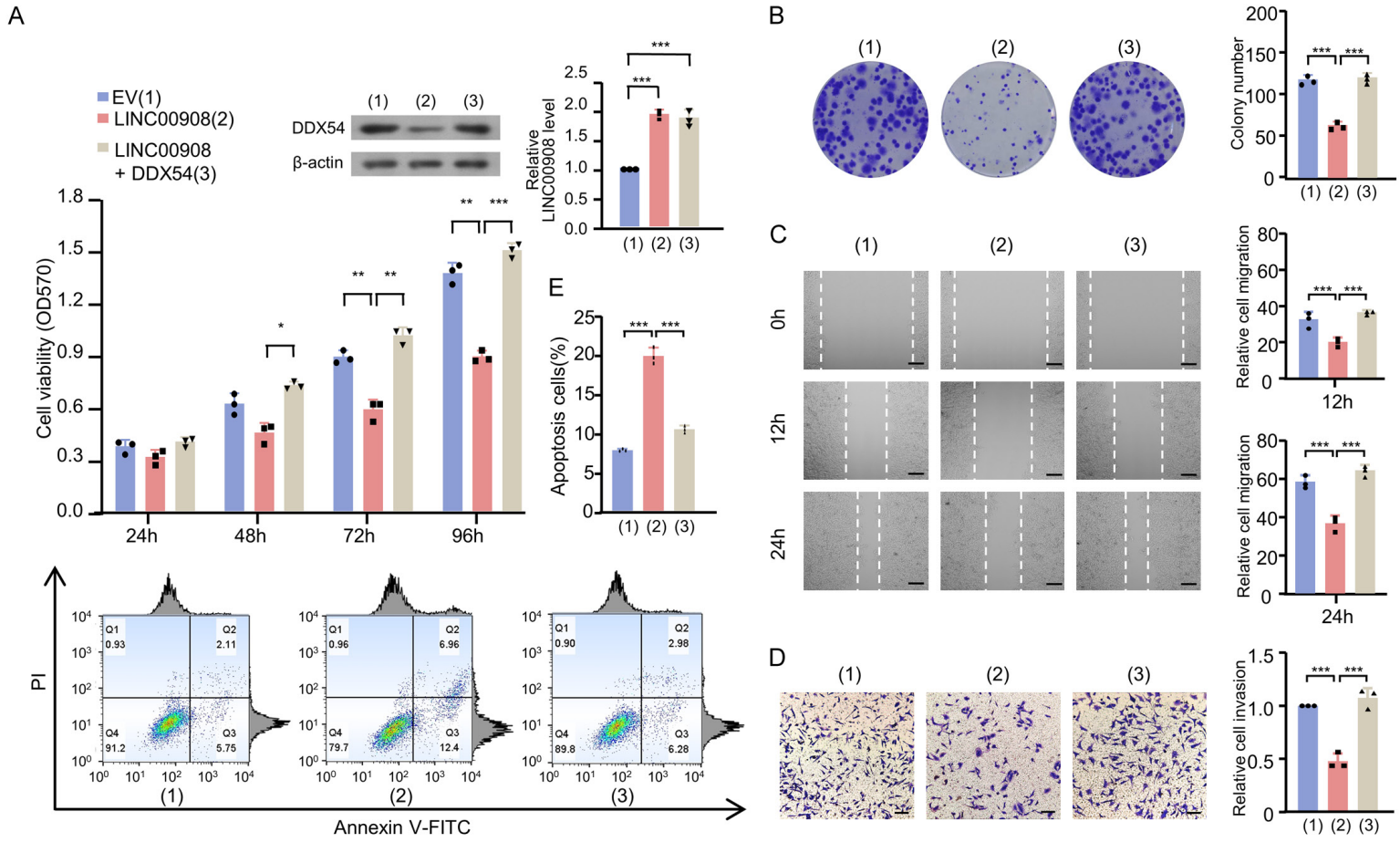
A
EV(1)
LINC00908(2)
LINC00908 + DDX54(3)
DDX54
β-actin
(1) (2) (3)
Relative LINC00908 level
Cell viability (OD570)
24h
48h
72h
96h
E
Apoptosis cells(%)
PI
Annexin V-FITC
B
Colony number
C
0h
12h
24h
Relative cell migration
D
Relative cell invasion

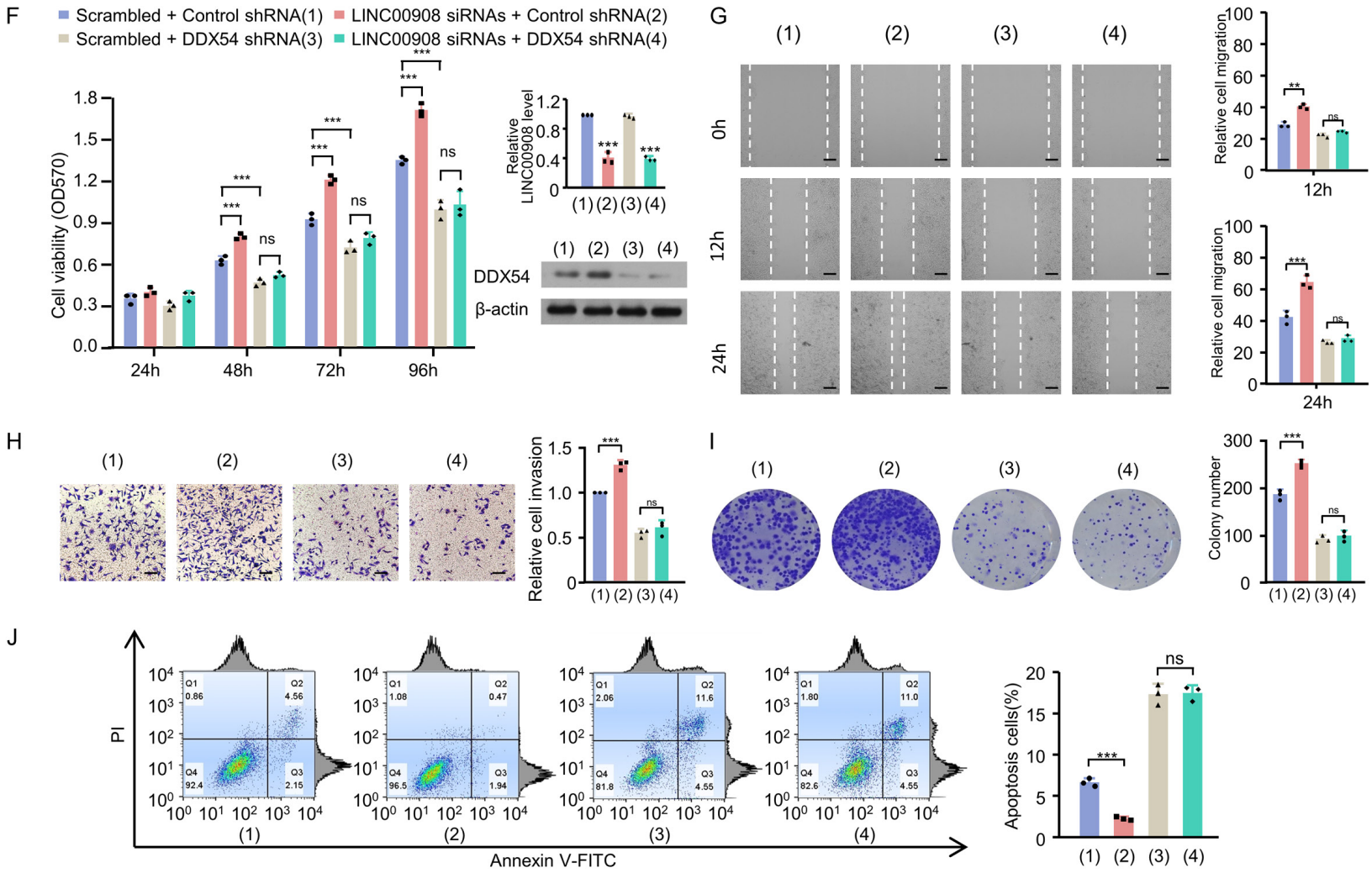

Figure 3. LINC00908/DDX54 regulated proliferation, migration, invasion and apoptosis in A549 cells. (A) A549 cells were transfected with empty vector (1) or LINC00908 (2) or LINC00908 plus DDX54 (3). The representative immunoblot shows DDX54 expression. LINC00908 expression was determined by qRT-PCR. Histograms shows the proliferation of A549 cells. (B) Colony-formation assay of A549 cells transfected as in (A). (C and D) Cell migration and invasion A549 cells transfected as in (A) were tested. (E) Cell apoptosis in A549 cells were evaluated by flow cytometry. (F) Proliferation of A549 cells transfected with scramble plus control shRNA (1) or LINC00908 siRNAs plus control shRNA (2) or scramble plus DDX54 shRNA (3) or LINC00908 siRNAs plus DDX54 shRNA (4). (G-J) Colony-formation, cell migration, invasion and apoptosis of A549 cells transfected as in (F) were tested. Histograms show colony number, comparative cell migration and invasion, and percentage of apoptosis cells. Scale bar = 50 μm. *P < 0.05, **P < 0.001, ***P < 0.0001.

Supplementary Figure 3A). Next, CCK8, apoptosis, wound healing, colony assay and transwell assays were conducted. As shown, LINC00908 overexpression inhibited the proliferation, migration, and invasion in both A549 and H1299 cells. Moreover, apoptosis assays indicated that overexpression of LINC00908 could accelerate cell apoptosis. Further, co-transfection with DDX54 and LINC00908 abolished these effects generated by LINC00908 overexpression (**Figure 3B-E**, Supplementary Figure 3B-E).

Conversely, LINC00908 knockdown notably enhanced the ability of proliferation, migration, invasion and downregulated cell apoptosis. DDX54 consistently restrained these effects of LINC00908 knockdown (**Figure 3F-J**, Supplementary Figure 3F-J). Collectively, these data demonstrate that LINC00908 dampens the growth, migration and invasion through its regulation of DDX54 in LUAD cells. Overexpression of LINC00908 could restrain LUAD progression, and its role as tumor suppressor is exerted possibly through regulating DDX54 expression in LUAD cells.

DDX54 knockdown downregulated glycolysis in LUAD cells

We also conducted Gene Set Variation Analysis (GSVA) analysis to detect the relationship between DDX54 and glycolysis-related pathways. There were 6 pathways implicated in glycolysis, involving KEGG_GLYCOLYSIS_GLUCONEOGENESIS, REACTOME_GLYCOLYSIS, WINTER_HYPOXIA_UP, MOOTHA_GLYCOLYSIS, WINTER_HYPOXIA_DN, GROSS_HYPOXIA_VIA_HIF1A_UP, QI_HYPOXIA_TARGETS_OF_HIF1A_AND_FOXA2 (**Figure 4A-C**, Supplementary Figure 4).

Additionally, we investigated the possible correlations between DDX54 and 12 glycolysis-related genes according to TCGA database. Strong positive correlations were detected between DDX54 and 11 genes (SLC2A1, HK2, GPI, PFKL, ALDOA, GAPDH, PGK1, PGAM1, ENO1, PKM, and LDHA) (**Figure 4D**, **4E**). We further found that DDX54 knockdown downregulated the mRNA and protein expression of SLC2A1, GPI, PFKL, ALDOA, PGK1, PGAM1, ENO1, PKM in both LUAD cells. We used a DDX54 plasmid designed to resist knockdown effects, with the sequence provided in Supplementary Table 2. Excitingly, these outcomes were reversed via re-expression of DDX54 in DDX54 knockdown cells (**Figure 4F**, **4G**), substantiating the role of DDX54 in glycolysis. Moreover, there was a decrease in ECAR and an increase in OCR with DDX54 knockdown, indicating lower glycolytic flux and higher mitochondrial respiration. Once more, DDX54 re-expression reversed these effects (**Figure 4H**, **4I**). Besides, glucose uptake, lactate production, ATP generation, and pyruvate were tested to evaluate the glycolysis level. As expected, DDX54 knockdown decreased glucose uptake, lactate production, ATP generation, and pyruvate, while DDX54 re-expression reversed these effects (**Figure 4J**, **4K**). To sum up, these data suggest that DDX54 knockdown downregulates glycolysis in both A549 and H1299 cells.

LINC00908 downregulated glycolysis through DDX54 in vitro

Since we proved the regulatory relationship between LINC00908 and DDX54, we next explored whether LINC00908 plays an important role in regulating glycolysis. GSVA analysis revealed that LINC00908 was negatively correlated with KEGG_GLYCOLYSIS_GLUCONEOGENESIS, REACTOME_GLYCOLYSIS, WINTER_HYPOXIA_UP, GROSS_HYPOXIA_VIA_HIF1A_UP, REACTOME_REGULATION_OF_GLYCOLYSIS_BY_FRUCTOSE_2_6_BISPHOSPHATE_METABOLISM (**Figure 5A-C**, Supplementary Figure 5). In vitro, LINC00908 knockdown upregulated the mRNA and protein levels of DDX54, SLC2A1, GPI, PFKL, ALDOA, PGK1, PGAM1, ENO1, PKM. DDX54 knockdown abolished these effects in both cells (**Figure 5D**, **5E**, **5I**, **5K**). Moreover, the results of glucose uptake, lactate production, ATP generation, pyruvate, ECAR and OCR also confirmed the effects of LINC00908 inhibiting glycolysis via DDX54 (**Figure 5F-H**, **5J**, **5L**, **5M**).

RFX2 was screened as one of the transcript factors for LINC00908

We predicted 383 transcription factors which may bind to the promoter region of LINC00908 using the bioinformatics database. These predicted transcription factors were then overlapped with the results of DEGs from the analysis results based on TCGA database. Finally, we obtained 40 candidate transcription factors (**Figure 6A**), of which 28 were associated to positive prognostic impact in LUAD. Among

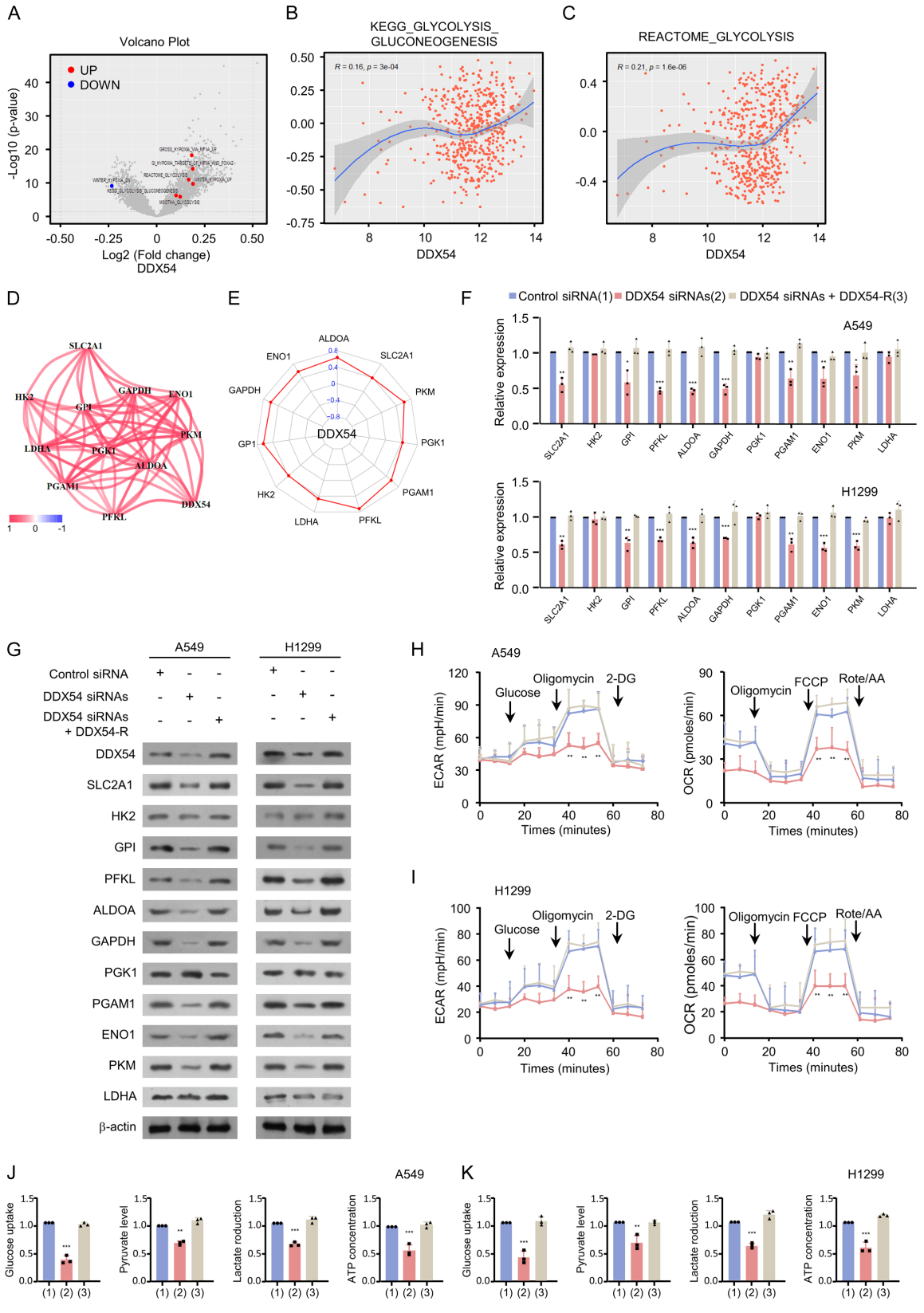

Figure 4. DDX54 knockdown downregulated glycolysis in LUAD cells. (A) 1 downregulated and 6 upregulated glycolysis related pathways between high and low DDX54 group as indicated by GSVA analysis. (B) The relationship between DDX54 expression and KEGG_GLYCOLYSIS_GLUCONEOGENESIS. (C) The relationship between DDX54

expression and REACTOME_GLYCOLYSIS. (D and E) The correlation coefficient between DDX54 expression level and 11 glycolysis-related genes. (F and G) The mRNA and protein levels of 11 glycolysis-related genes in A549 and H1299 cells transfected with control siRNA (1) or DDX54 siRNAs (2) or DDX54 siRNAs plus DDX54-R (3). (H-K) ECAR, OCR, Glucose uptake, Pyruvate, Lactate production and ATP production were measured in A549 and H1299 cells transfected as in (F). *P < 0.05, **P < 0.001, ***P < 0.0001.

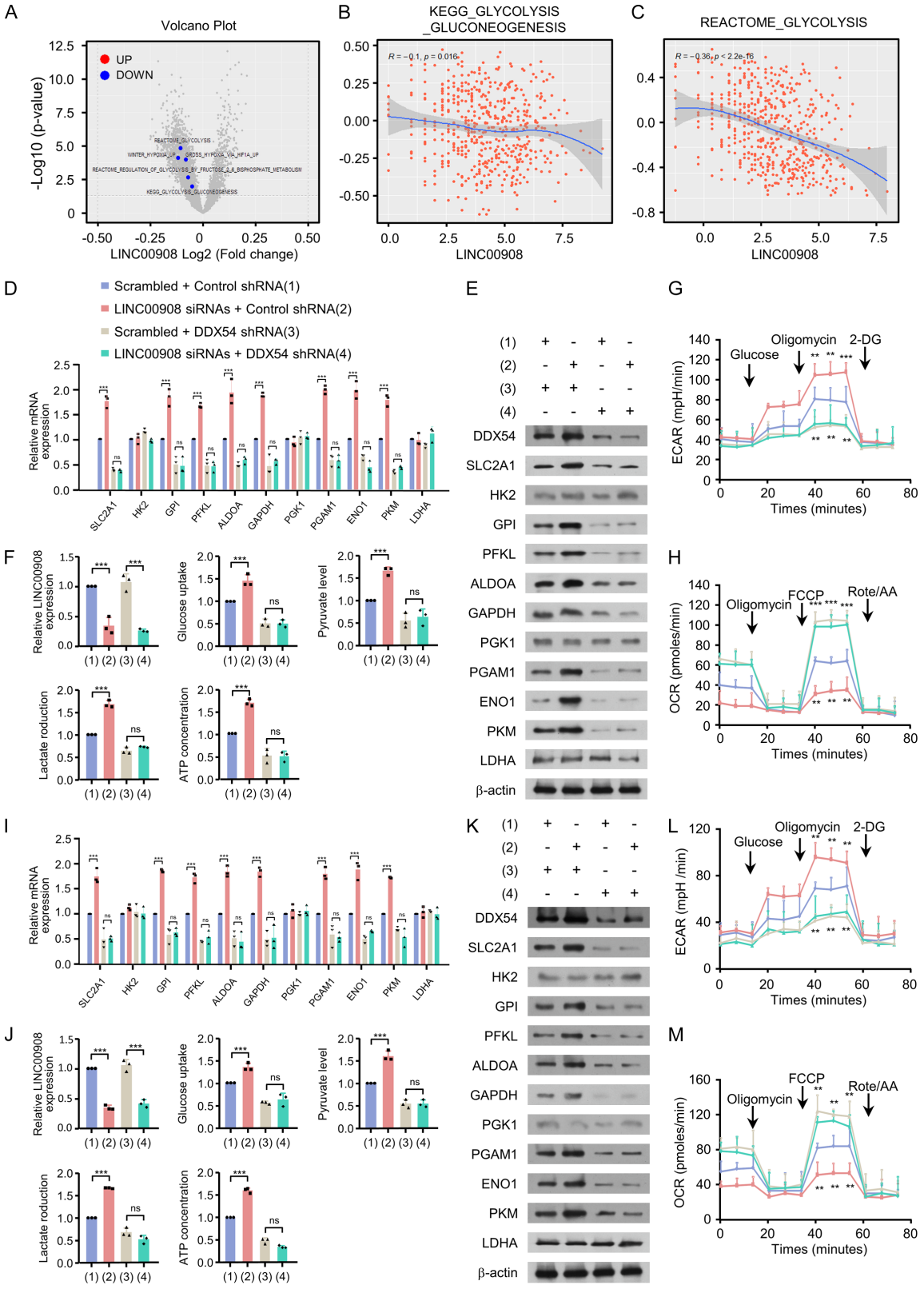

Figure 5. LINC00908 downregulated glycolysis through DDX54 in vitro. (A) There are 5 downregulated glycolysis related pathways between high and low LINC00908 groups by GSVA analysis. (B) The relationship between LINC00908 expression and KEGG_GLYCOLYSIS_GLUCONEOGENESIS. (C) The relationship between DDX54 expression and REACTOME_GLYCOLYSIS. (D, E, I and K) The mRNA and protein levels of 11 glycolysis-related genes in A549 and H1299 cells transfected with scramble plus control shRNA (1) or LINC00908 siRNAs plus control shRNA (2) or scramble plus DDX54 siRNAs (3) or LINC00908 siRNAs plus DDX54 siRNAs (4). (F-H, J, L and M) ECAR, OCR, Glucose uptake, Pyruvate, Lactate production and ATP production were measured in A549 and H1299 cells transfected as in (D). *P < 0.05, **P < 0.001, ***P < 0.0001.

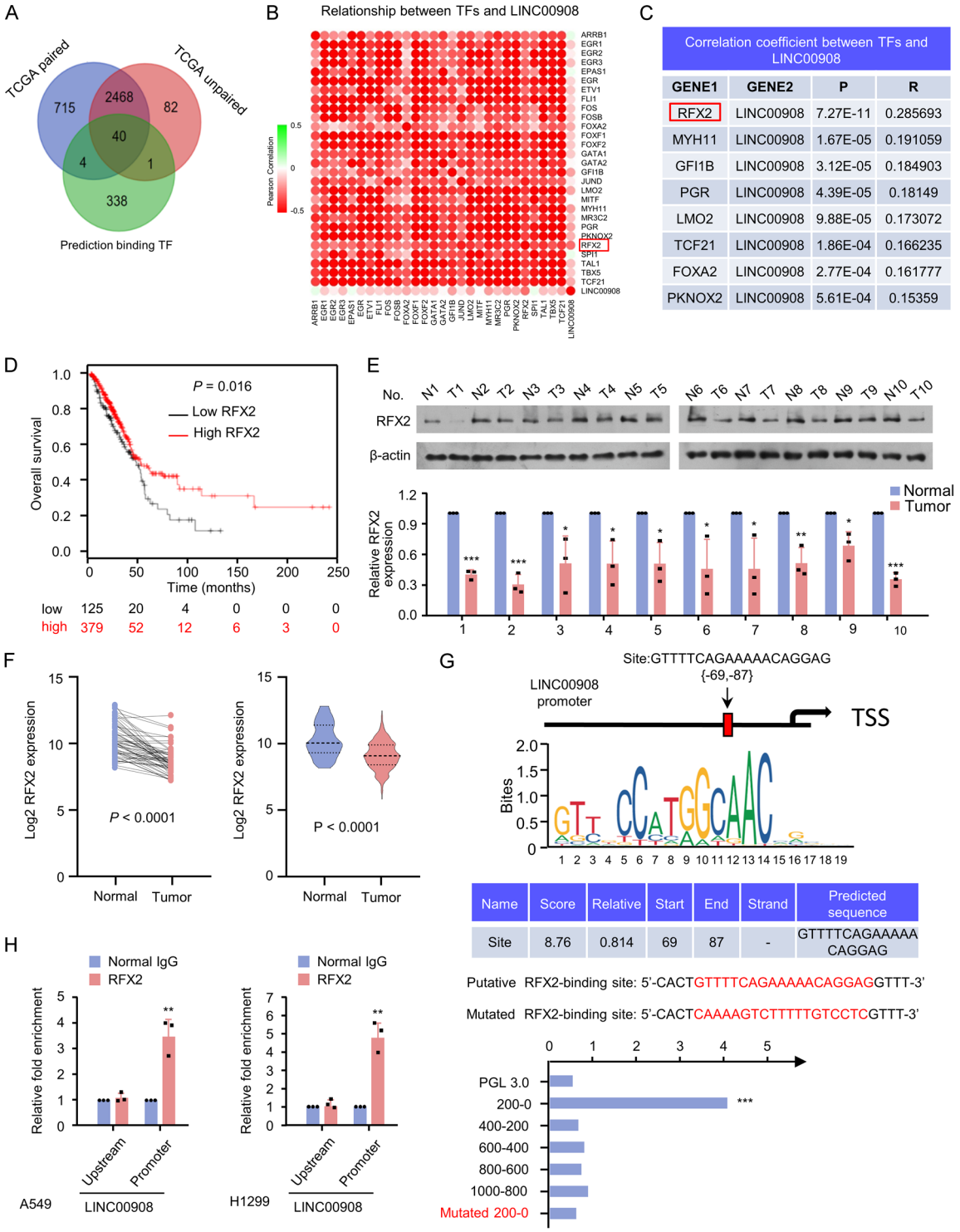

Figure 6. RFX2 was screened as one of the transcript factors (TFs) for LINC00908. A. Venn analysis of the DEGs and predicted TFs. The overlapped circle of purple and red represents the DEGs in paired and unpaired LUAD tissues. The green circle represents the predicted TFs targeting LINC00908 by online analysis (https://jaspar.genereg.net/). The intersection of the results revealed 40 TFs. B. The correlation matrix between LINC00908 expression and 28 positive prognosis transcript factors in LUAD. C. The correlation coefficient between LINC00908 expression and the most relevant 8 transcription factors using Pearson analysis. D. Kaplan-Meier estimate of OS in terms of RFX2 in LUAD patients from TCGA (http://kmplot.com/analysis/). E. RFX2 expression in 10 paired tumor and adjacent normal tissues were detected using real-time RT-PCR and Western-blot. F. RFX2 expression between tumor and adjacent normal tissues in TCGA database were displayed. G. A conserved RFX2-binding element at the LINC00908 promoter was predicted by JASPAR (http:/jaspar.genereg.net). Luciferase activity of different LINC00908 promoter reporters in A549 cells. H. CHIP analysis of RFX2 occupancy on the LINC00908 promoter or upstream in A549 and H1299 cells. *P < 0.05, **P < 0.001, ***P < 0.0001.

these, RFX2 is of particular interest, for its significant correlations with LINC00908 (**Figure 6B-D**). Based on the important role of RFX2 in LUAD, we then detected the mRNA and protein expression of RFX2 in 10 pairs of tumor and adjacent tissues. The results demonstrated that RFX2 expression was significantly lower in tumor tissues than that in adjacent tissues (**Figure 6E**). Similar results were confirmed in paired or unpaired LUAD samples from TCGA database (**Figure 6F**). Thus, it is of importance to further investigate the specific association between RFX2 and LINC00908. We predicted the expected binding sites by a bioinformatics tool (http://jaspar.genereg.net/). Experiments demonstrated that RFX2 overexpression increased the luciferase activity of LINC00908 promoter containing the putative RFX2-binding site, whereas the effect was little on the promoter presenting mutated binding site (**Figure 6G**). Consistent with this, chromatin immunoprecipitation (ChIP) assay showed that RFX2 was proved to bind to the LINC00908 promoter, not upstream (**Figure 6H**). These results suggest RFX2 as one of the critical transcription factors for LINC00908.

RFX2 mediated proliferation, apoptosis, migration, invasion and glycolysis by regulating LINC00908 in LUAD cells

Subsequently, we validated the possible association between RFX2 and LINC00908 in regulation of LUAD progressions. The results showed that RFX2 overexpression inhibited LUAD cell growth, while LINC00908 knockdown led to RFX2 inactivation in regulating cell proliferation (**Figure 7A**, **7B**, Supplementary Figure 6A and 6B). We further explored whether RFX2 affected cell apoptosis, migration, and invasion via LINC00908. As expected, RFX2 overexpression inhibited LUAD cell migration and invasion, and accelerated cell apoptosis. LINC00908 knockdown greatly dampened these effects of RFX2 overexpression (**Figure 7C-E**, Supplementary Figure 6C-E).

We also detected the functions of RFX2 on glycolysis in LUAD. RFX2 overexpression suppressed mRNA and protein expression levels of DDX54 and glycolytic genes, including SLC2A1, GPI, PFKL, ALDOA, GAPDH, PGAM1, ENO1, and PKM. Moreover, these functions of RFX2 were abolished by LINC00908 knockdown (**Figure 7F**, **7G**; Supplementary Figure 6F, 6G). Corresponding with the above results, RFX2 overexpression displayed decreased ECAR and increased OCR, which were abolished by LINC00908 knockdown (**Figure 7H**, **7I**; Supplementary Figure 6H, 6I). Further studies also revealed that RFX2 dampened glucose uptake, lactate production, ATP generation, and pyruvate ratio. This reduction could also be reversed by LINC00908 knockdown (**Figure 7J**; Supplementary Figure 6J). Taken together, these data imply that RFX2 suppresses LUAD cell growth, migration, invasion, glycolysis, and accelerates apoptosis, largely dependent on LINC00908.

RFX2/LINC00908/DDX54 axis has a tumor-promoting effect in vivo

We next aimed to investigate the phenotype of the RFX2/LINC00908/DDX54 pathway *in vivo*. First, BALB/c nude mice were subcutaneously injected with A549 cells engineered with specific constructs. We detected that LINC00908 knockdown significantly elevated LUAD tumor growth, whereas knockdown of DDX54 blocked tumor growth. These results highlighted the regulatory role of LINC00908 in modulating tumor growth through DDX54 (**Figure 8A-D**). Next, we examined the important roles of RFX2 and LINC00908 in the regulation of LUAD tumor growth. As shown in **Figure 8E-H**, RFX2 overexpression significantly decreased LUAD tumor growth, while this effect was dramatical-

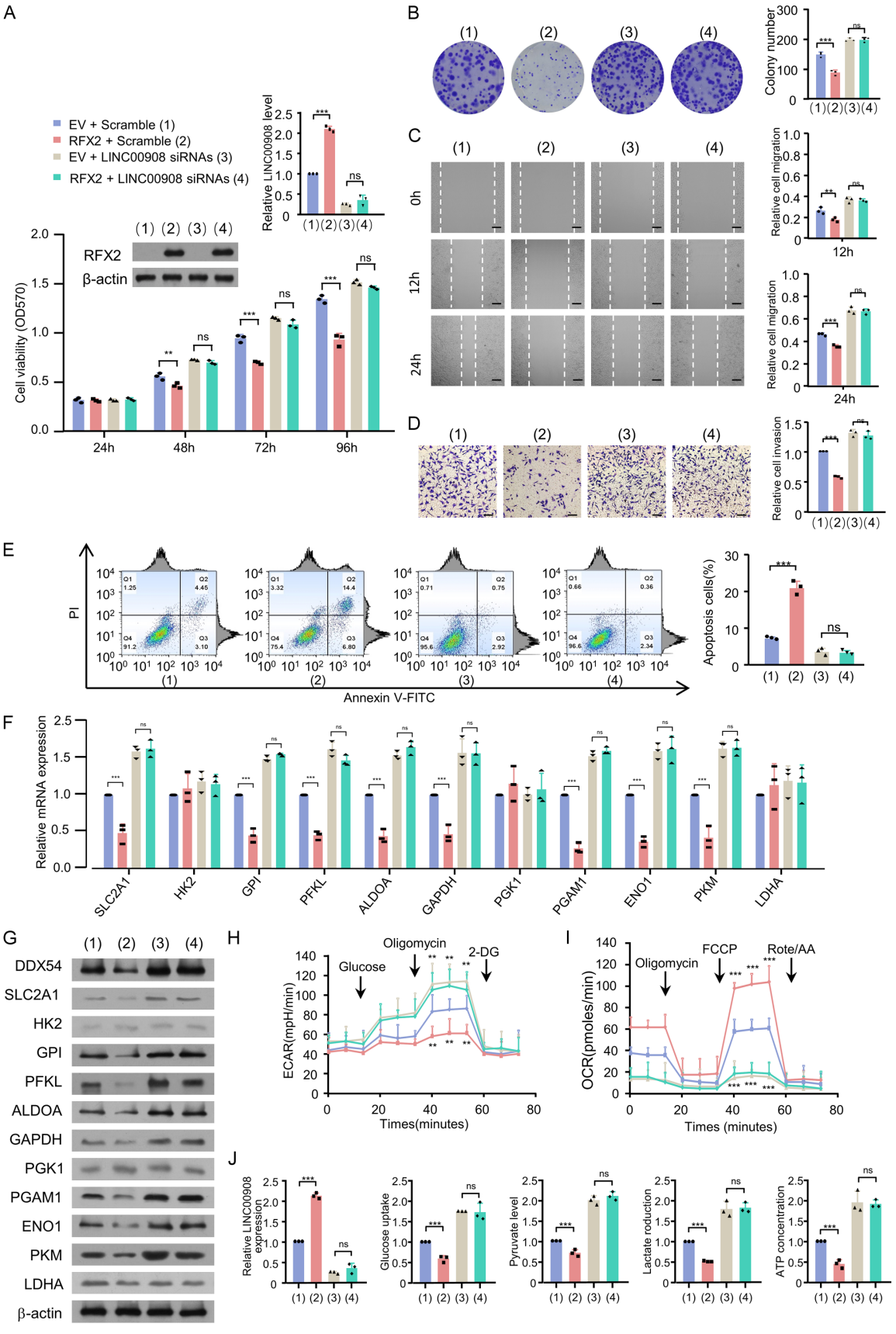
A
EV + Scramble (1)
RFX2 + Scramble (2)
EV + LINC00908 siRNAs (3)
RFX2 + LINC00908 siRNAs (4)
Relative LINC00908 level
RFX2
β-actin
Cell viability (OD570)
24h
48h
72h
96h
B
Colony number
C
0h
12h
24h
Relative cell migration
D
Relative cell invasion
E
PI
Annexin V-FITC
Apoptosis cells(%)
F
Relative mRNA expression
SLC2A1
HK2
GPI
PFKL
ALDOA
GAPDH
PGK1
PGAM1
ENO1
PKM
LDHA
G
DDX54
SLC2A1
HK2
GPI
PFKL
ALDOA
GAPDH
PGK1
PGAM1
ENO1
PKM
LDHA
β-actin
H
Glucose
Oligomycin
2-DG
ECAR(mpH/min)
Times(minutes)
I
Oligomycin
FCCP
Rote/AA
OCR(pmoles/min)
Times (minutes)
J
Relative LINC00908 expression
Glucose uptake
Pyruvate level
Lactate roduction
ATP concentration

Figure 7. RFX2 suppressed proliferation, apoptosis, migration, invasion and glycolysis by regulating LINC00908 in A549 cells. (A) A549 cells were transfected with empty vector plus scramble (1) or RFX2 plus scramble (2) or empty vector plus LINC00908 siRNAs (3) or RFX2 plus LINC00908 siRNAs (4). The immunoblot shows RFX2 in the 4 groups. LINC00908 knockdown lead to RFX2 inactivation in regulating cell proliferation. (B-E) Colony-formation, cell migration, invasion, and apoptosis of A549 cells transfected as in (A). Histograms show proliferation, colony number, comparative cell migration and invasion, and percentage of apoptosis cells. (F and G) A549 cells were transfected with empty vector plus scramble (1) or RFX2 plus scramble (2) or empty vector plus LINC00908 siRNAs (3) or RFX2 plus LINC00908 siRNAs (4). The mRNA and protein levels of 11 glycolysis-related genes were measured. (H-J) ECAR, OCR, Glucose uptake, Pyruvate, Lactate production and ATP production were detected. Scale bar = 50 μm. *P < 0.05, **P < 0.001, ***P < 0.0001.

ly attenuated when LINC00908 was knocked down. These data suggest the key role of RFX2/LINC00908/DDX54 axis *in vivo*.

Clinical relevance of LINC00908, DDX54 and RFX2 in the LUAD patients

We performed immunohistochemical (IHC) staining to assess DDX54 expression and FISH assays to examine LINC00908 expression in 130 human LUAD samples. Positive correlation was found between LINC00908 expression and RFX2 expression, but negative correlation with DDX54 expression (**Figure 8I**, **8J**). The potential regulatory pathway is shown in **Figure 8K**. Overall, these results indicate that RFX2/LINC00908/DDX54 axis is likely to play important pathological roles in LUAD.

Discussion

Enhanced glycolysis is recognized as a metabolic characteristic of numerous cancers, affected by several key factors, including hypoxia, ubiquitination, and metabolic stress [19-21]. Recently, LncRNAs have been increasingly reported to function as promoting or suppressing roles in glycolytic pathway [22, 23]. For example, in LUAD, LINC00857 regulated the cell glycolysis mainly through targeting the miR-1179/SPAG5 [24]. LncRNA FAM83A-AS1 contributed to cell proliferation and stemness via the HIF-1α/glycolysis axis [25]. Cao *et al*. identified four critical glycolysis-related LncRNAs associated with prognosis [26]. Therefore, searching for new LncRNAs that target glycolysis in LUAD is of great significance.

LINC00908 is a recently identified lncRNA. Wang *et al*. demonstrated that LINC00908 downregulation was associated with poor OS in TNBC and encoded a polypeptide, ASRPS [27]. Shan *et al*. showed that LINC00908 was significantly upregulated, promoted proliferation and inhibited apoptosis of colorectal cancer cells by regulating KLF5 expression [28]. However, the clinical values and detail roles of LINC00908 in LUAD progression remain largely unknown. Our data suggest multiple functions of LINC00908 that contribute to tumorigenesis in LUAD. In this study, we first delineated the critical role of LINC00908 in regulating LUAD growth and progression. More importantly, LINC00908 suppresses aerobic glycolysis in LUAD cells through inhibition of DDX54 expression.

Several DDX family members are known to regulate mRNA translation in cancer cells, and inhibitors targeting DDX proteins are currently under development. DDX54 was reported to play a cancerous role in colorectal cancer [29]. Our data suggest that high DDX54 expression predicts poor PFS and OS in LUAD patients. In addition, co-transfection of DDX54 and LINC00908 abolished the ability of LINC00908 to regulate LUAD cell proliferation, migration, invasion, and glycolysis. The molecular and functional interaction between DDX54 and LINC00908 described in our report represents a critical mechanism in LUAD.

Recent studies have shown that dysregulation of LncRNA is associated with oncogenic transcription factors [30]. Investigations of the function of regulatory factor X (RFX) have shown that RFX regulates genes involved in various cellular and developmental processes. Dysregulation of RFX is highly associated with severe disease [31]. RFX2 was identified as one of the master transcription factors in regulating angiogenesis signature in kidney renal clear cell carcinoma patients [32]. In our study, RFX2 was confirmed to regulate the expression of LINC00908, and 2 predicted binding sites for RFX2 in the LINC00908 promoter were proved. Here we explored a mechanism of RFX2 in controlling LUAD cell growth and inhibiting glycolysis through upregulation of LINC00908 expression. Based on these find-

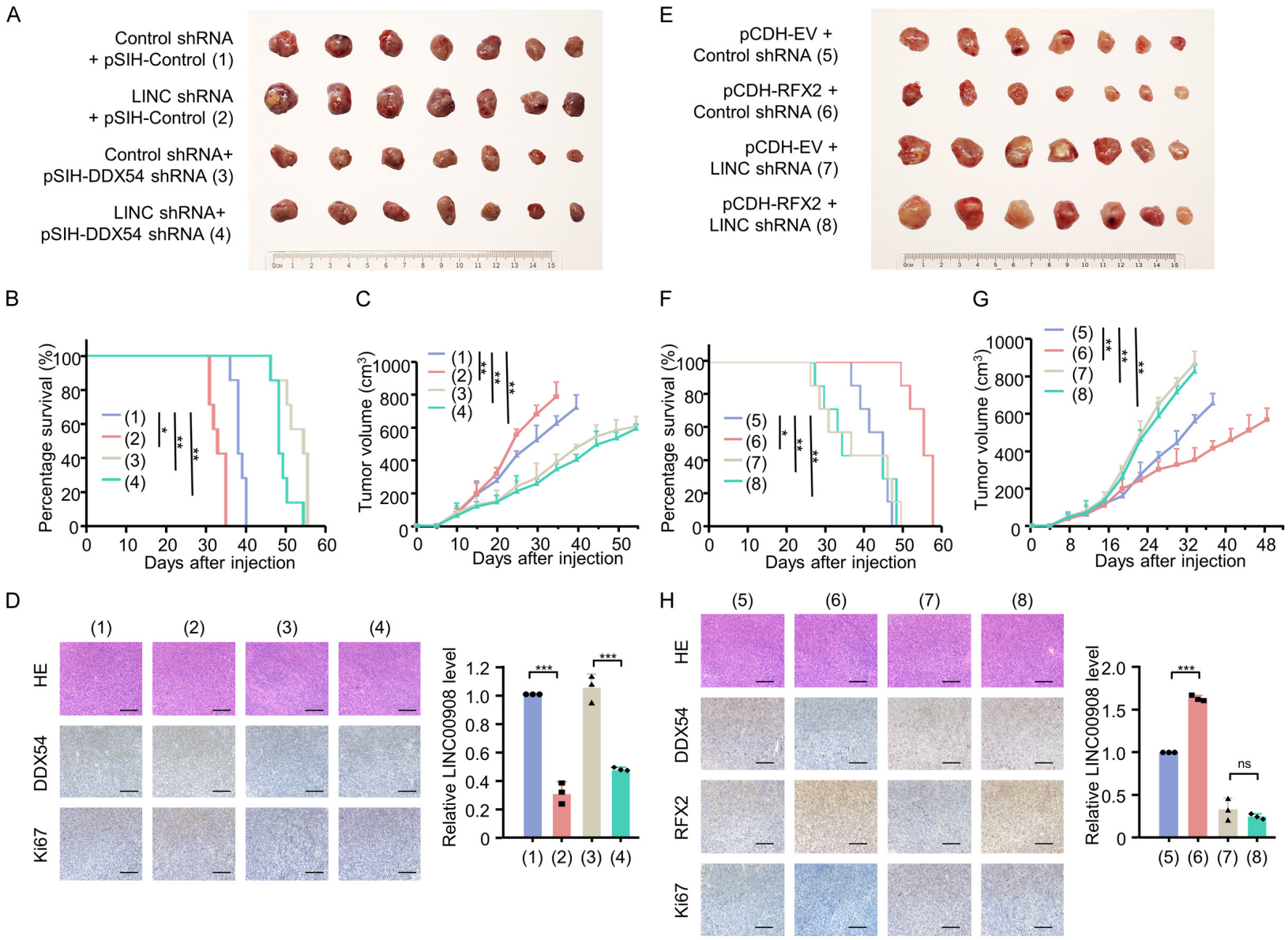
A
Control shRNA
+ pSIH-Control (1)
LINC shRNA
+ pSIH-Control (2)
Control shRNA+
pSIH-DDX54 shRNA (3)
LINC shRNA+
pSIH-DDX54 shRNA (4)
E
pCDH-EV +
Control shRNA (5)
pCDH-RFX2 +
Control shRNA (6)
pCDH-EV +
LINC shRNA (7)
pCDH-RFX2 +
LINC shRNA (8)
B
Percentage survival (%)
Days after injection
C
Tumor volume (cm3)
Days after injection
F
Percentage survival (%)
Days after injection
G
Tumor volume (cm3)
Days after injection
D
HE
DDX54
Ki67
Relative LINC00908 level
H
HE
DDX54
RFX2
Ki67
Relative LINC00908 level
ns

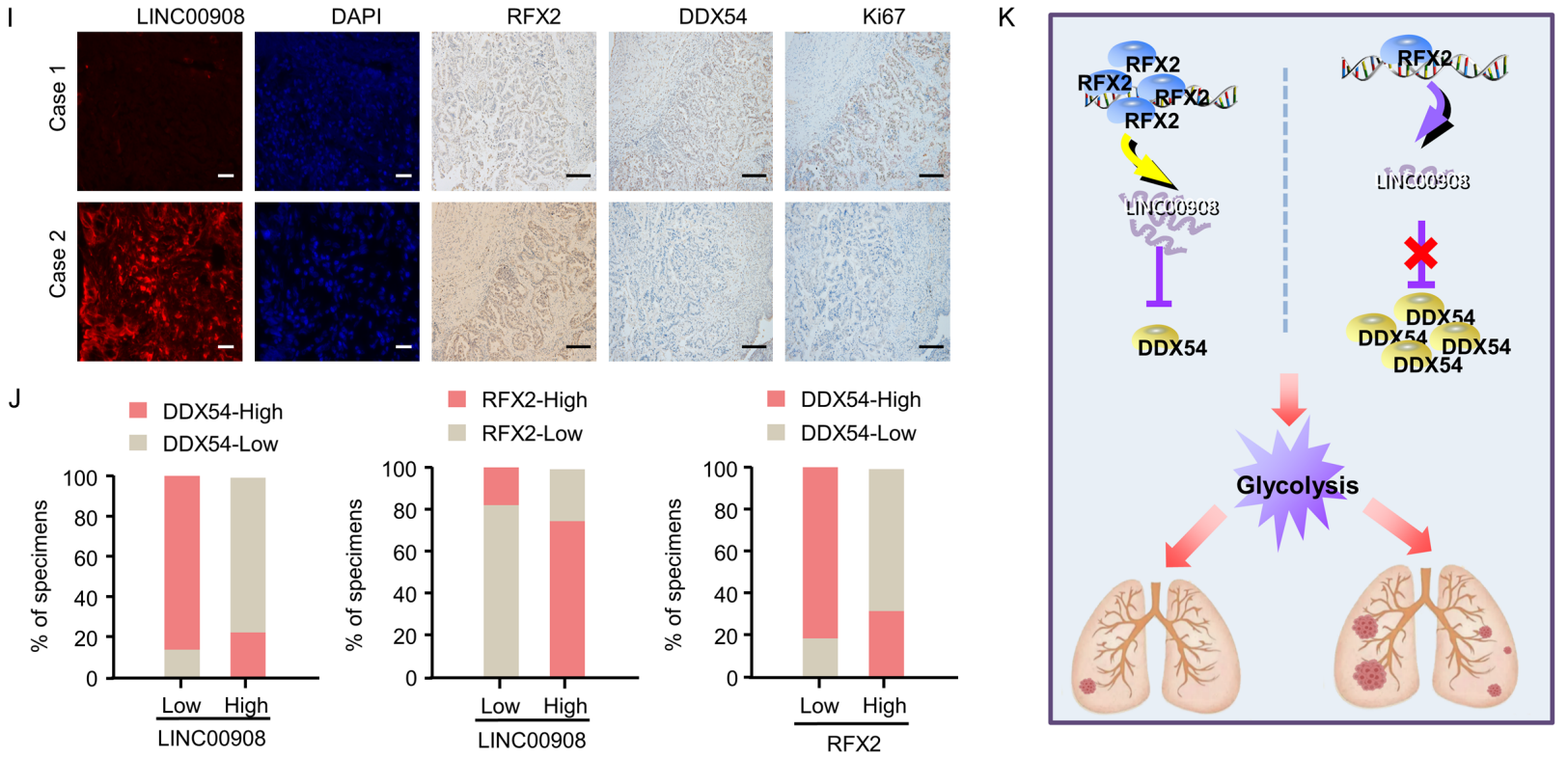

Figure 8. RFX2/LINC00908/DDX54 axis has a tumor-promoting effect *in vivo* and their expression in human LUAD tissues. A and E. Representative images of tumors from the BALB/c nude mice subcutaneously inoculated with A549 cells expressing the indicated constructs. B and F. Representative HE staining. C, D, G and H. Survival and growth curve were measured and plotted. All data were presented as the mean ± SEM (n = 7 per group). Scale bar = 50 μm. I. Representative FISH staining for LINC00908 and IHC staining for RFX2, DDX54, ki67 in LUAD patients. Scale bar = 50 μm. J. Correlation among LINC00908, DDX54 and RFX2 in terms of the specimen percentage. K. Schematic of the regulatory network of LUAD in this study.

ings, we speculate that RFX2/LINC00908/DDX54 axis has critical biological functions in LUAD.

In conclusion, our study reveals a distinctive mechanism regulating LINC00908 in LUAD. RFX2/LINC00908/DDX54 axis regulates LUAD cell proliferation, migration, invasion and glycolysis in vitro and in vivo, which is a potential therapeutic target for the prevention and treatment of LUAD.

Acknowledgements

This work was supported by the Sixth Medical Center of PLA General Hospital Innovation Cultivation Fund (CXPY202201).

Disclosure of conflict of interest

None.

Address correspondence to: Xiangyang Chu, Department of Thoracic Surgery, The First Medical Center, Chinese PLA General Hospital and Chinese PLA Medical School, Beijing, China. E-mail: drchu301301@163.com; Yang Zhang, Department of Cardiology, The Second Medical Center, Chinese PLA General Hospital, Beijing, China. E-mail: olivianna@163.com; Xiao Han, Department of Oncology, The Fifth Medical Center, Chinese PLA General Hospital and Chinese PLA Medical School, Beijing, China. E-mail: hanxiaoplagh@126.com

References

[1] Siegel RL, Miller KD, Fuchs HE and Jemal A. Cancer statistics, 2022. CA Cancer J Clin 2022; 72: 7-33.
[2] Wu F, Wang L and Zhou C. Lung cancer in China: current and prospect. Curr Opin Oncol 2021; 33: 40-46.
[3] Succony L, Rassl DM, Barker AP, McCaughan FM and Rintoul RC. Adenocarcinoma spectrum lesions of the lung: detection, pathology and treatment strategies. Cancer Treat Rev 2021; 99: 102237.
[4] Faubert B, Li KY, Cai L, Hensley CT, Kim J, Zacharias LG, Yang C, Do QN, Doucette S, Burguete D, Li H, Huet G, Yuan Q, Wigal T, Butt Y, Ni M, Torrealba J, Oliver D, Lenkinski RE, Malloy CR, Wachsmann JW, Young JD, Kernstine K and DeBerardinis RJ. Lactate metabolism in human lung tumors. Cell 2017; 171: 358-371, e359.
[5] Hanahan D. Hallmarks of cancer: new dimensions. Cancer Discov 2022; 12: 31-46.
[6] Li L, Liang Y, Kang L, Liu Y, Gao S, Chen S, Li Y, You W, Dong Q, Hong T, Yan Z, Jin S, Wang T, Zhao W, Mai H, Huang J, Han X, Ji Q, Song Q, Yang C, Zhao S, Xu X and Ye Q. Transcriptional regulation of the warburg effect in cancer by SIX1. Cancer Cell 2018; 33: 368-385, e367.
[7] Hu Y, Mu H and Deng Z. The transcription factor TEAD4 enhances lung adenocarcinoma progression through enhancing PKM2 mediated glycolysis. Cell Biol Int 2021; 45: 2063-2073.
[8] Kopp F and Mendell JT. Functional classification and experimental dissection of long noncoding RNAs. Cell 2018; 172: 393-407.
[9] Peng WX, Koirala P and Mo YY. LncRNA-mediated regulation of cell signaling in cancer. Oncogene 2017; 36: 5661-5667.
[10] Jia M, Li Z, Pan M, Tao M, Wang J and Lu X. LINC-PINT suppresses the aggressiveness of thyroid cancer by downregulating miR-767-5p to induce TET2 expression. Mol Ther Nucleic Acids 2020; 22: 319-328.
[11] Yang Z, Dong X, Pu M, Yang H, Chang W, Ji F, Liu T, Wei C, Zhang X and Qiu X. LBX2-AS1/miR-219a-2-3p/FUS/LBX2 positive feedback loop contributes to the proliferation of gastric cancer. Gastric Cancer 2020; 23: 449-463.
[12] Xu X, Chen X, Shen X, Chen R, Zhu C, Zhang Z, Chen Y, Lin W, Xu X, Lin Y and Lai Z. Genome-wide identification and characterization of DEAD-box helicase family associated with early somatic embryogenesis in Dimocarpus longan Lour. J Plant Physiol 2021; 258-259: 153364.
[13] Karmakar S, Rauth S, Nallasamy P, Perumal N, Nimmakayala RK, Leon F, Gupta R, Barkeer S, Venkata RC, Raman V, Rachagani S, Ponnusamy MP and Batra SK. RNA polymerase II-associated factor 1 regulates stem cell features of pancreatic cancer cells, independently of the PAF1 complex, via interactions with PHF5A and DDX3. Gastroenterology 2020; 159: 1898-1915, e1896.
[14] Yang P, Li J, Peng C, Tan Y, Chen R, Peng W, Gu Q, Zhou J, Wang L, Tang J, Feng Y and Sun Y. TCONS_00012883 promotes proliferation and metastasis via DDX3/YY1/MMP1/PI3K-AKT axis in colorectal cancer. Clin Transl Med 2020; 10: e211.
[15] Zhang M, Weng W, Zhang Q, Wu Y, Ni S, Tan C, Xu M, Sun H, Liu C, Wei P and Du X. The lncRNA NEAT1 activates Wnt/beta-catenin signaling and promotes colorectal cancer progression via interacting with DDX5. J Hematol Oncol 2018; 11: 113.
[16] Milek M, Imami K, Mukherjee N, Bortoli F, Zinnall U, Hazapis O, Trahan C, Oeffinger M, Heyd F, Ohler U, Selbach M and Landthaler M. DDX54 regulates transcriptome dynamics dur-

ing DNA damage response. Genome Res 2017; 27: 1344-1359.
[17] Paine I, Posey JE, Grochowski CM, Jhangiani SN, Rosenheck S, Kleyner R, Marmorale T, Yoon M, Wang K, Robison R, Cappuccio G, Pinelli M, Magli A, Coban Akdemir Z, Hui J, Yeung WL, Wong BKY, Ortega L, Bekheirnia MR, Bierhals T, Hempel M, Johannsen J, Santer R, Aktas D, Alikasifoglu M, Bozdogan S, Aydin H, Karaca E, Bayram Y, Ityel H, Dorschner M, White JJ, Wilichowski E, Wortmann SB, Casella EB, Kitajima JP, Kok F, Monteiro F, Muzny DM, Bamshad M, Gibbs RA, Sutton VR; University of Washington Center for Mendelian Genomics, Baylor-Hopkins Center for Mendelian Genomics, Telethon Undiagnosed Diseases Program; Van Esch H, Brunetti-Pierri N, Hildebrandt F, Brautbar A, Van den Veyver IB, Glass I, Lessel D, Lyon GJ and Lupski JR. Paralog studies augment gene discovery: DDX and DHX genes. Am J Hum Genet 2019; 105: 302-316.
[18] Zhang Y, Guo H and Zhang H. SNHG10/DDX54/PBX3 feedback loop contributes to gastric cancer cell growth. Dig Dis Sci 2021; 66: 1875-1884.
[19] Abbaszadeh Z, Cesmeli S and Biray Avcı C. Crucial players in glycolysis: cancer progress. Gene 2020; 726: 144158.
[20] Abdel-Wahab AF, Mahmoud W and Al-Harizy RM. Targeting glucose metabolism to suppress cancer progression: prospective of anti-glycolytic cancer therapy. Pharmacol Res 2019; 150: 104511.
[21] Xie Y, Wang M, Xia M, Guo Y, Zu X and Zhong J. Ubiquitination regulation of aerobic glycolysis in cancer. Life Sci 2022; 292: 120322.
[22] Bhan A, Soleimani M and Mandal SS. Long noncoding RNA and cancer: a new paradigm. Cancer Res 2017; 77: 3965-3981.
[23] Lin W, Zhou Q, Wang CQ, Zhu L, Bi C, Zhang S, Wang X and Jin H. LncRNAs regulate metabolism in cancer. Int J Biol Sci 2020; 16: 1194-1206.
[24] Wang L, Cao L, Wen C, Li J, Yu G and Liu C. LncRNA LINC00857 regulates lung adenocarcinoma progression, apoptosis and glycolysis by targeting miR-1179/SPAG5 axis. Hum Cell 2020; 33: 195-204.
[25] Chen Z, Hu Z, Sui Q, Huang Y, Zhao M, Li M, Liang J, Lu T, Zhan C, Lin Z, Sun F, Wang Q and Tan L. LncRNA FAM83A-AS1 facilitates tumor proliferation and the migration via the HIF-1alpha/glycolysis axis in lung adenocarcinoma. Int J Biol Sci 2022; 18: 522-535.
[26] Cao P, Zhao B, Xiao Y, Hu S, Kong K, Han P, Yue J, Deng Y, Zhao Z, Wu D, Zhang L and Li F. Understanding the critical role of glycolysis-related lncRNAs in lung adenocarcinoma based on three molecular subtypes. Biomed Res Int 2022; 2022: 7587398.
[27] Wang Y, Wu S, Zhu X, Zhang L, Deng J, Li F, Guo B, Zhang S, Wu R, Zhang Z, Wang K, Lu J and Zhou Y. LncRNA-encoded polypeptide ASRPS inhibits triple-negative breast cancer angiogenesis. J Exp Med 2020; 217: jem.20190950.
[28] Shan TD, Tian ZB, Li Q, Jiang YP, Liu FG, Sun XG, Han Y, Sun LJ and Chen L. Long intergenic noncoding RNA 00908 promotes proliferation and inhibits apoptosis of colorectal cancer cells by regulating KLF5 expression. J Cell Physiol 2021; 236: 889-899.
[29] Yu Y, Wang JL, Meng LL, Hu CT, Yan ZW, He ZP, Shi XQ, Fu GH and Zu LD. DDX54 plays a cancerous role through activating P65 and AKT signaling pathway in colorectal cancer. Front Oncol 2021; 11: 650360.
[30] Long Y, Wang X, Youmans DT and Cech TR. How do lncRNAs regulate transcription? Sci Adv 2017; 3: eaao2110.
[31] Sugiaman-Trapman D, Vitezic M, Jouhilahti EM, Mathelier A, Lauter G, Misra S, Daub CO, Kere J and Swoboda P. Characterization of the human RFX transcription factor family by regulatory and target gene analysis. BMC Genomics 2018; 19: 181.
[32] Zheng W, Zhang S, Guo H, Chen X, Huang Z, Jiang S and Li M. Multi-omics analysis of tumor angiogenesis characteristics and potential epigenetic regulation mechanisms in renal clear cell carcinoma. Cell Commun Signal 2021; 19: 39.

Supplementary Table 1. The primers for real-time PCR

Gene	Forward primer (5' to 3')	Reverse primer (5' to 3')
LINC00908	TGCACCGGTTTCATCGGTCTG	TTACATACGTAATGACTTTCTTGTC
DDX54	GGAATTCTACATCCCCTACCG	CCACTTCTGATAGAGGTCTC
β-actin	GGGACCTGACTGACTACCTC	TCATACTCCTGCTTGCTGAT
SLC2A1	CATCCCATGGTTCATCGTGGC	GAAGTAGGTGAAGATGAAGAACA
HK2	GAGCCACCACTCACCCTACT	CCAGGCATTCGGCAATGTG
GPI	CAAGGACCGCTTCAACCACTT	CCAGGATGGGTGTGTTTGACC
PFKL	GCTGGGCGGCACTATCATT	TCAGGTGCGAGTAGGTCCG
ALDOA	ATGCCCTACCAATATCCAGCA	GCTCCCAGTGGACTCATCTG
GAPDH	GGAGCGAGATCCCTCCAAAAT	GGCTGTTGTCATACTTCTCATGG
PGK1	TGGACGTTAAAGGGAAGCGG	GCTCATAAGGACTACCGACTTGG
PGAM1	GTGCAGAAGAGAGCGATCCG	CGGTTAGACCCCCATAGTGC
ENO1	AAAGCTGGTGCCGTTGAGAA	GGTTGTGGTAAACCTCTGCTC
PKM	GACCCGGAATCCCCAGACAG	TCACGGCACAGGAACAACACG
LDHA	ATGGCAACTCTAAAGGATCAGC	CCAACCCCAACAACTGTAATCT

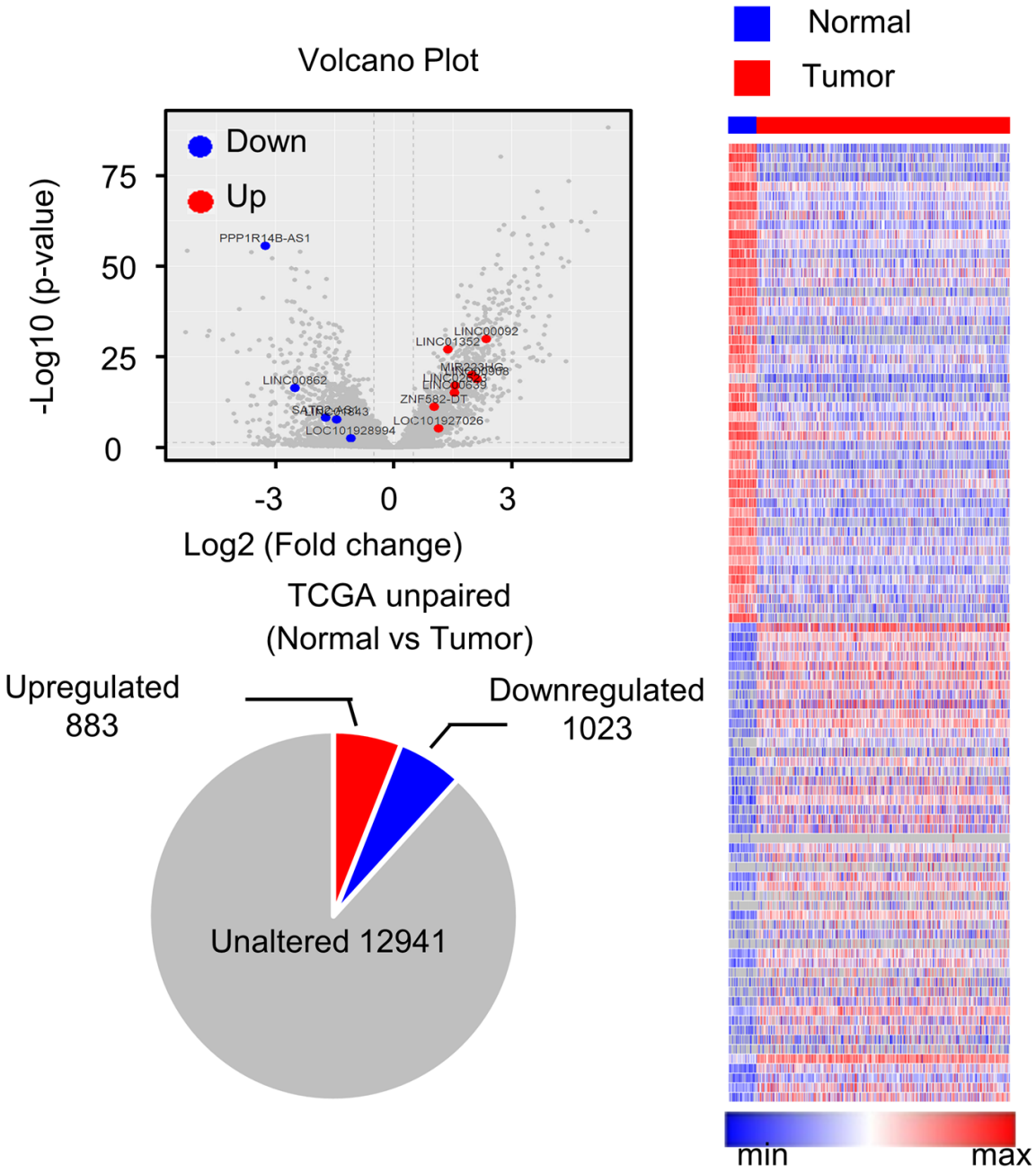

Supplementary Figure 1. A volcano plot illustrating differentially regulated LncRNA expressions between unpaired normal and tumor LUAD tissues based on TCGA database. Values are presented as the log10 of tag counts. Pie chart revealed a total of 14847 genes expressed, of which 883 genes were upregulated and 1023 genes were downregulated. The hierarchical clustering of the RNA-seq analysis results shows all genes that were significantly differently expressed.

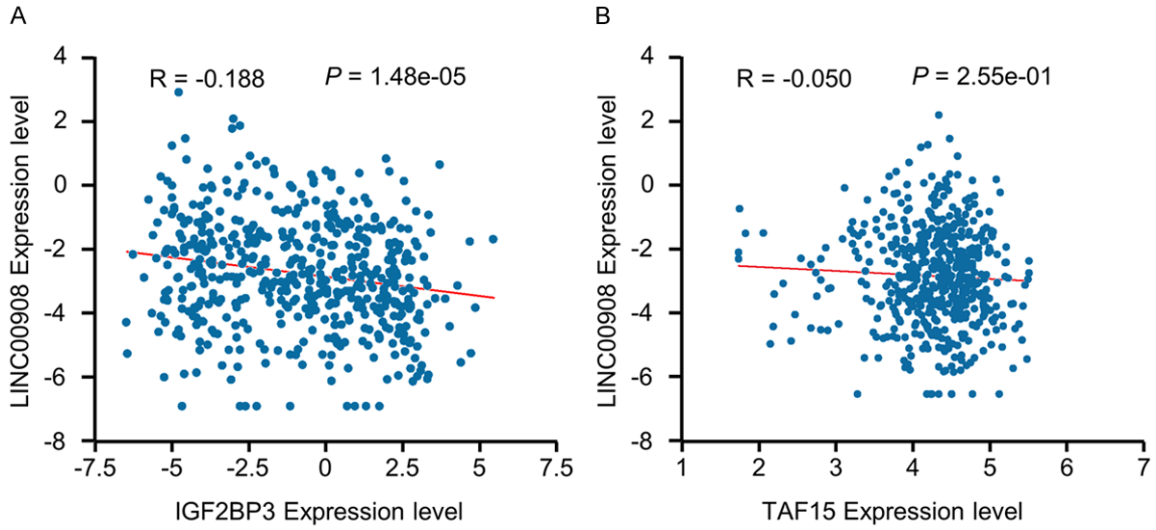

Supplementary Figure 2. A and B. The relationship between the expression of LINC00908 and IGF2BP3 or TAF15 in LUAD based on TCGA database by online analysis (https://starbase.sysu.edu.cn).

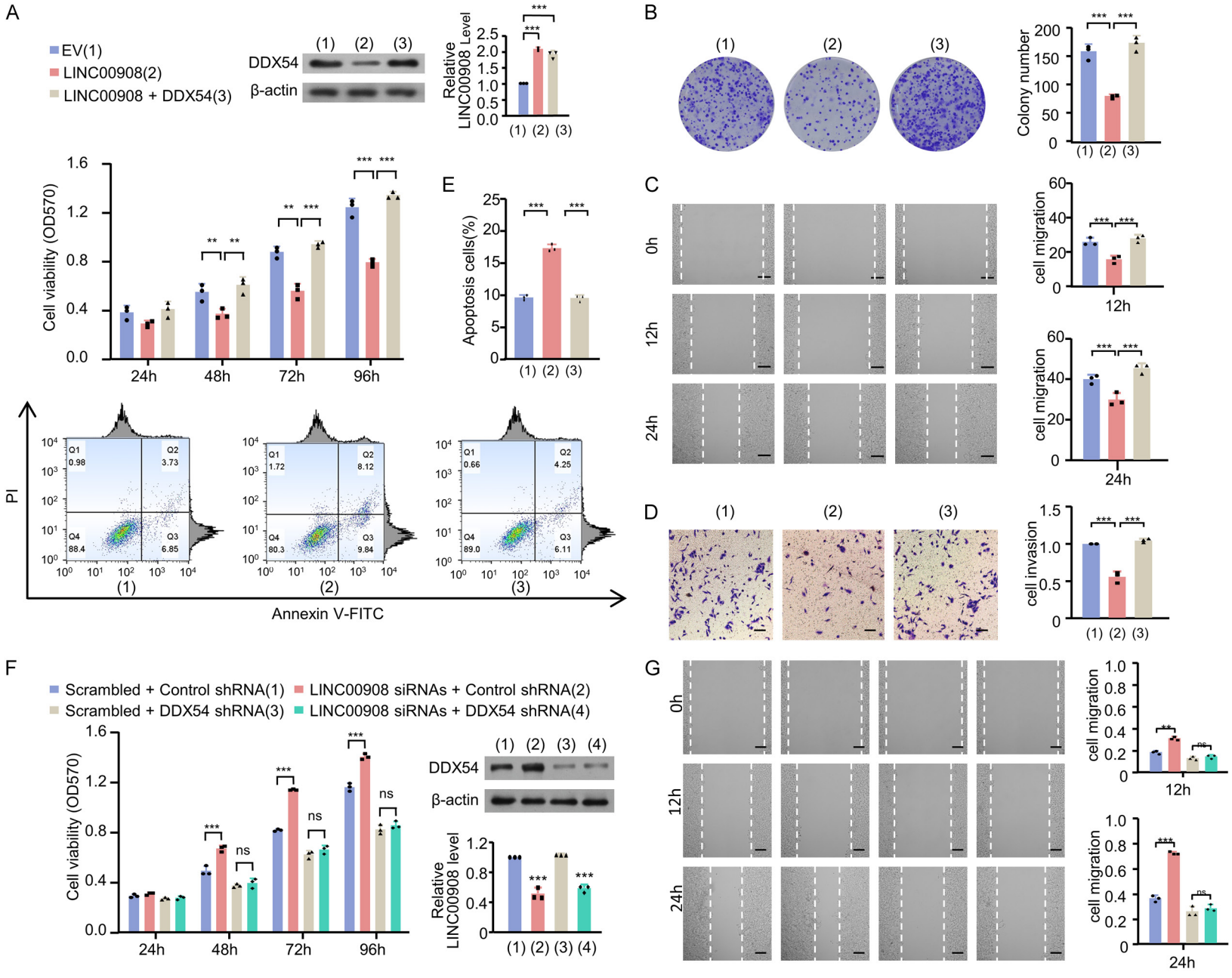
A
EV(1)
LINC00908(2)
LINC00908 + DDX54(3)
DDX54
β-actin
(1) (2) (3)
Relative LINC00908 Level
Cell viability (OD570)
24h 48h 72h 96h
B
Colony number
C
0h
12h
24h
cell migration
D
cell invasion
E
Apoptosis cells(%)
PI
Annexin V-FITC
Q1 0.98
Q2 3.73
Q4 88.4
Q3 6.85
Q1 1.72
Q2 8.12
Q4 80.3
Q3 9.84
Q1 0.66
Q2 4.25
Q4 89.0
Q3 6.11
F
Scrambled + Control shRNA(1)
LINC00908 siRNAs + Control shRNA(2)
Scrambled + DDX54 shRNA(3)
LINC00908 siRNAs + DDX54 shRNA(4)
(1) (2) (3) (4)
G

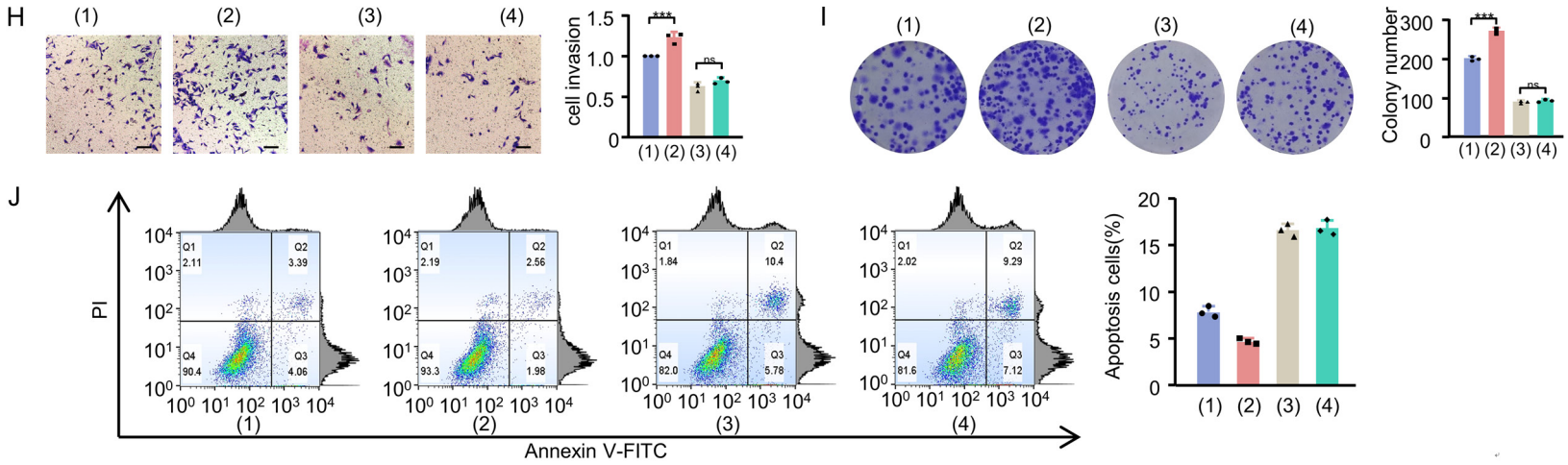

Supplementary Figure 3. LINC00908/DDX54 regulated proliferation, migration, invasion and apoptosis in H1299 cells. (A) H1299 cells were transfected with empty vector (1) or LINC00908 (2) or LINC00908 plus DDX54 (3). The representative immunoblot shows DDX54 expression. LINC00908 expression were determined by qRT-PCR. Histograms showed the proliferation of H1299 cells. (B) Colony-formation assay of H1299 cells transfected as in (A). (C and D) Cell migration and transwell assays of invasion H1299 cells transfected as in (A) were tested. (E) Cell apoptosis in H1299 cells were evaluated by flow cytometry. (F) H1299 cells proliferation transfected with scramble plus control shRNA (1) or LINC00908 siRNAs plus control shRNA (2) or scramble plus DDX54 shRNA (3) or LINC00908 siRNAs plus DDX54 shRNA (4). (G-J) Colony-formation, cell migration, invasion and apoptosis in H1299 cells transfected as in (F) were tested. Histograms show colony number, comparative cell migration and invasion, and percentage of apoptosis cells. Scale bar = 50 μm.*P < 0.05, **P < 0.001, ***P < 0.0001.

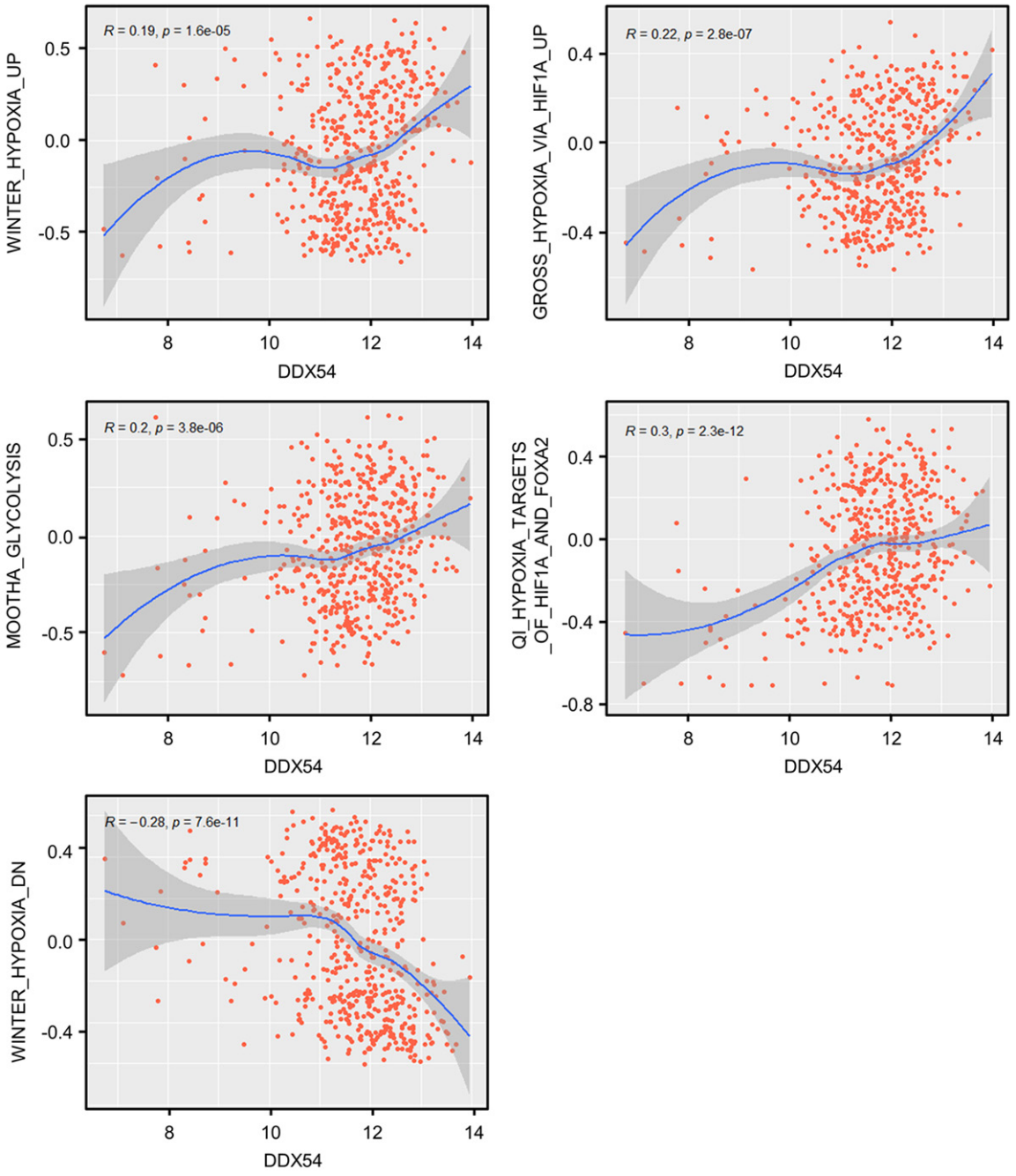

Supplementary Figure 4. The relationship between DDX54 expression and WINTER_HYPOXIA_UP or MOOTHA_GLYCOLYSIS or WINTER_HYPOXIA_DN or GROSS_HYPOXIA_VIA_HIF1A_UP or QI_HYPOXIA_TARGETS_OF_HIF1A_AND_FOXA2.

Supplementary Table 2. The sequences of DDX54-R

ATGGCGGCCGACAAGGGCCCGGCGGCTGGACCTCGGTCGCGAGCTGCCATGGCCCAGTGGAGGAAGAAGAAAGGGCTCCG-
GAAGCGCCGAGGCGCGGCCTCCCAGGCCCGCGGCAGCGACTCGGAGGACGGCGAGTTTGAGATCCAGGCGGAAGATGAC-
GCCCGGGCCCGGAAGCTGGGACCTGGAAGACCCCTGCCCACCTTCCCCACCTCGGAATGCACCTCGGATGTGGAGCCGGA-
CACCCGGGAGATGGTGCGTGCCCAGAACAAGAAGAAGAAGAAGTCTGGAGGCTTCCAGTCCATGGGCCTGAGCTACCCGGT-
GTTTTAAAGGCATCATGAAGAAGGGGTACAAGGTGCCAACACCCATCCAGAGGAAGACCATCCCGGTGATCTTGGATGGCAAGGAC-
GTGGTGGCCATGGCCCGGACGGGCAGTGGCAAGACAGCCTGCTTCCTCCTCCCAATGTTCGAGCGGCTCAAGACCCACAGT-
GCCCAGACCGGGGCCCGCGCCCTCATCCTCTCGCCGACCCGAGAGCTGGCCCTGCAGACCCTGAAGTTCACTAAGGAGCTAG-
GCAAGTTCACTGGCCTCAAGACTGCCCTGATCCTGGGTGGAGACAGGATGGAAGACCAGTTTGCAGCCCTGCACGAAAATCCC-
GACATAATTATTGCCACGCCCGGACGGTTGGTGCATGTGGCTGTGGAAATGAGCCTGAAGCTGCAGAGTGTGGAATACGTGGT-
GTTCGATGAAGCTGACCGGCTTTTTGAAATGGGTTTCGCAGAGCAGCTGCAGGAGATCATCGCCCGCCTCCCCGGGGGCCAC-
CAGACGGTGCTGTTCTCCGCCACGCTGCCCAAACTGCTGGTGGAATTTGCCCGGGCTGGCCTCACGGAGCCCGTGCTCATC-
CGGCTTGACGTGGATACCAAGCTCAACGAGCAGCTGAAGACCTCCTTCTTCCTCGTGCGGGAGGACACCAAGGCTGCCGTGCT-
GCTCCACCTGCTGCACAACGTGGTGCGGCCCCAGGACCAGACCGTGGTGTTTGTGGCCACGAAGCACCACGCCGAGTACCT-
CACTGAGCTGCTGACGACCCAGCGGGTGAGCTGCGCCCACATCTACAGTGCCCTAGACCCGACAGCCCGCAAGATCAACCCTC-
GCCAAATTCACGCTTGGCAAGTGCTCCACTCTCATTGTGACTGACCTGGCCGCCCGAGGCCTGGACATCCCGCTGCTGGA-
CAATGTCATCAACTACAGCTTCCCCGCCAAGGGCAAACTCTTCCTGCACCGCGTGGGCCGTGTGGCTCGGGCTGGCCGAAGTG-
GCACAGCCTACTCCTTGGTGGCCCCTGATGAAATCCCCTACCTGCTGGATCTGCACCTGTTCCTGGGCCGCTCCCTCACCCTC-
GCCCGACCCCTCAAGGAGCCCTCAGGTGTGGCCGGTGTGGATGGCATGCTGGGTCGGGTGCCACAGAGTGTGGTGGACGAG-
GAGGACAGTGGTCTGCAGAGCACCCTGGAGGCATCGCTGGAGCTACGGGGCCTGGCCCGCGTTGCTGATAACGCCCAGCAG-
CAGTATGTGCGCTCACGCCCGGCGCCCTCGCCTGAGTCCATCAAGAGGGCCAAGGAGATGGACCTTGTGGGGCTGGGCCTG-
CACCCCCTCTTCAGCTCGCGTTTTGAGGAGGAGGAGCTGCAGCGGCTGAGGCTGGTGGACAGCATAAAGAACTACCGCTCCC-
GGGCGACTATCTTTGAGATCAACGCCTCCAGCCGAGACCTGTGCAGCCAGGTGATGCGCGCCAAGCGGCAGAAGGACCG-
CAAGGCCATCGCCCGCTTCCAGCAGGGACAGCAGGGGCGGCAGGAGCAGCAGGAGGGCCCAGTGGGCCCAGCCCCGAGC-
CGCCCAGCACTGCAGGAGAAGCAGCCTGAGAAGGAGGAGGAGGAGGAGGCGGGAGAGAGTGTGGAGGACATTTTCTCAGAG-
GTCGTGGGCCGGAAGCGGCAGCGGTCAGGACCCAACAGGGGAGCCAAGAGGCGGAGGGAGGAGGCCCGGCAGCGGGAC-
CAGGAATTCTACATCCCCTACCGGCCCAAGGACTTTGACAGCGAGCGGGGCCTGAGCATCAGCGGGGAAGGGGGAGCCTTT-
GAGCAGCAGGCAGCTGGCGCTGTCCTGGACTTGATGGGGGATGAAGCCCAGAACCTGACGAGGGGCCGGCAGCAGCT-
CAAGTGGGACCGTAAGAAGAAGCGGTTTGTGGGACAGTCAGGACAGGAAGACAAGAAGAAGATTAAGACAGAGAGCGGC-
CGCTACATAAGCAGCTCCTACAAGCGAGACCTCTATCAGAAGTGGAAACAGAAACAGAAAATTGATGATCGTGACTCGGAC-
GAAGAAGGGGCATCTGACCGGCGAGGCCCAGAGCGAAGAGGTGGGAAGCGAGACCGTGGCCAAGCAGGTGCATCCCG-
GCCCCACGCCCCAGGCACCCCTGCAGGCCGAGTCCGCCCGGAACTCAAGACCAAGCAGCAGATCCTGAAGCAGCGGCGC-
CGGGCCCAGAAGCTGCACTTCCTGCAGCGTGGTGGCCTCAAGCAGCTCTCTGCCCGCAACCGCCGCCGCGTCCAGGAGCTG-
CAGCAGGGCGCCTTCGGCCGGGGTGCCCGCTCCAAGAAGGGCAAGATGCGGAAGAGGATGTGA

The red font represents the target sequence of siRNAs and the yellow font represents the mutation sites.

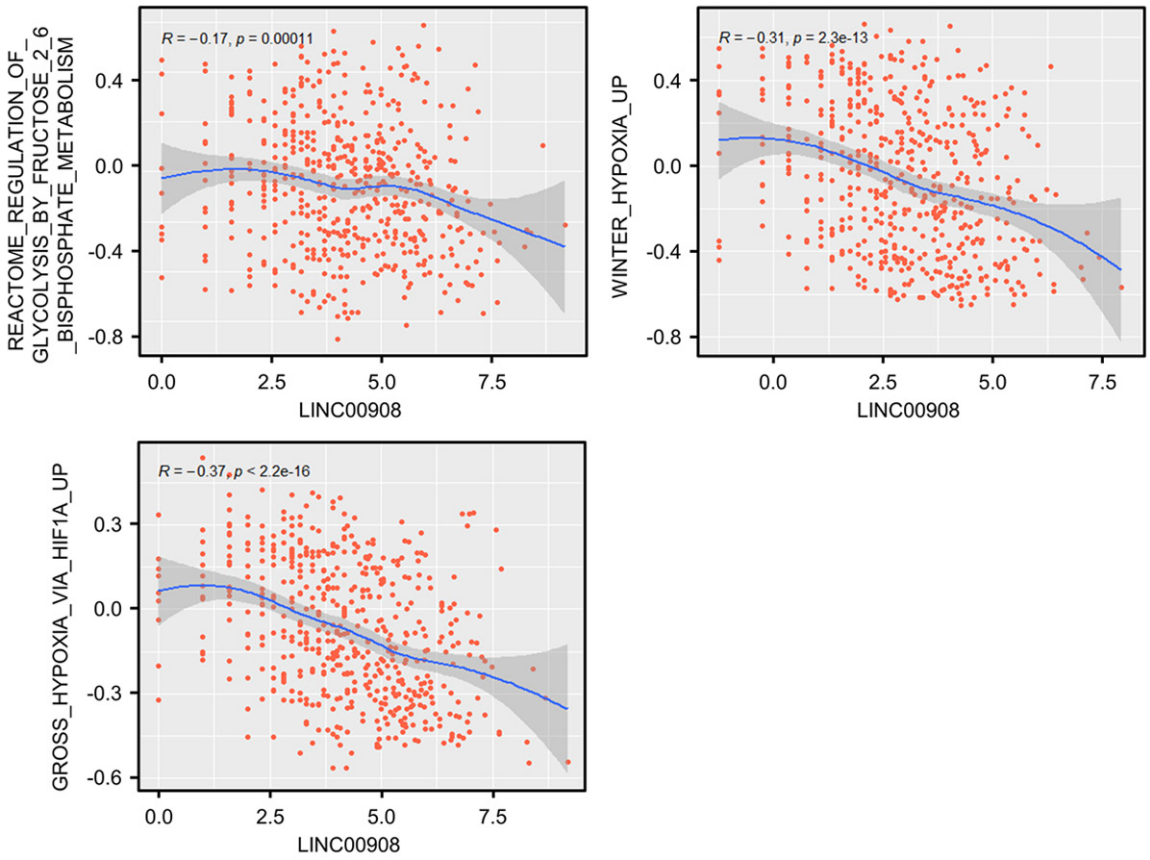

Supplementary Figure 5. The relationship between LINC00908 expression and REACTOME_REGULATION_OF_GLYCOLYSIS_BY_FRUCTOSE_2_6_BISPHOSPHATE_METABOLISM or WINTER_HYPOXIA_UP or GROSS_HYPOXIA_VIA_HIF1A_UP.

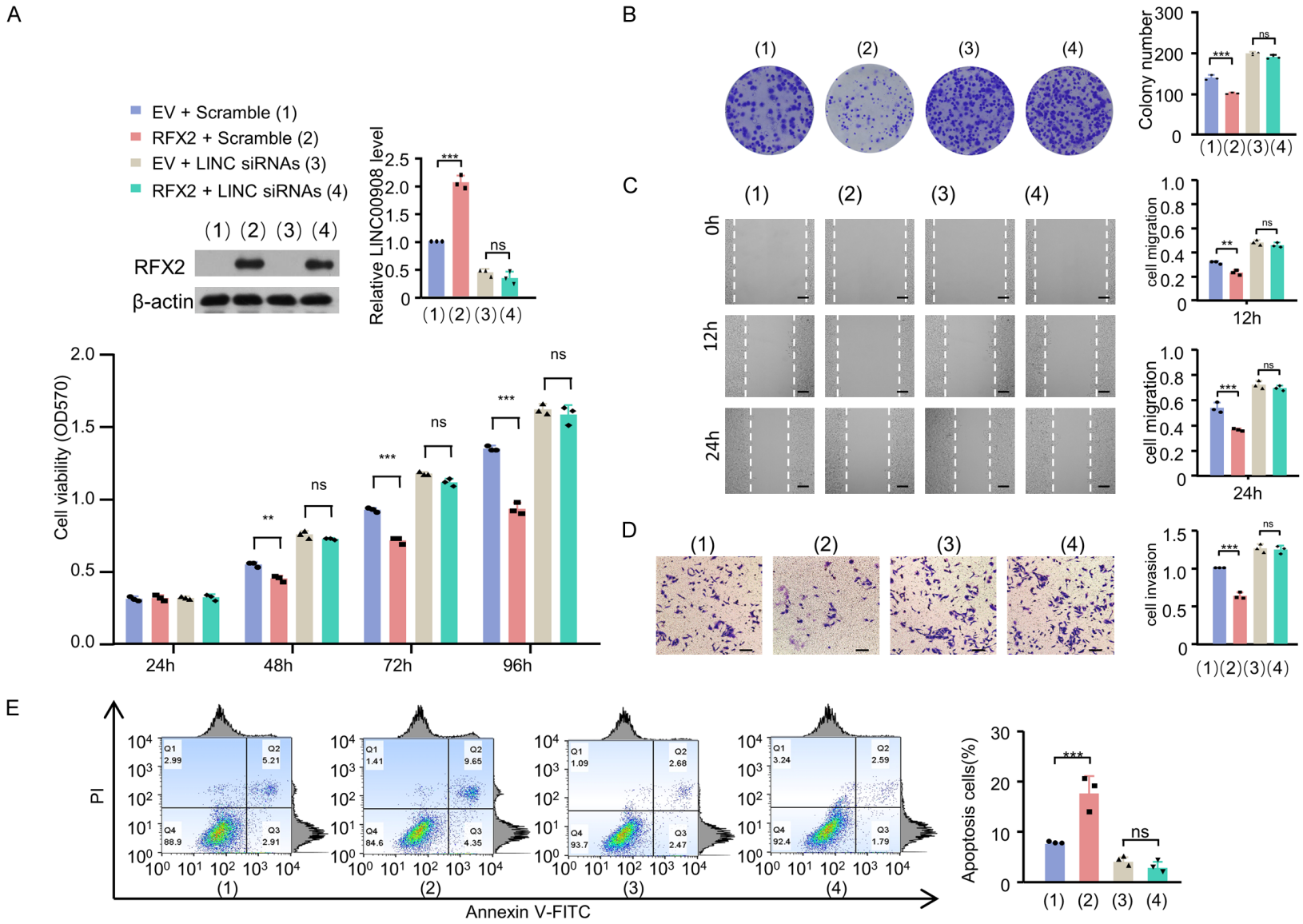
A
EV + Scramble (1)
RFX2 + Scramble (2)
EV + LINC siRNAs (3)
RFX2 + LINC siRNAs (4)
(1) (2) (3) (4)
RFX2
β-actin
Relative LINC00908 level
Cell viability (OD570)
24h
48h
72h
96h
B
Colony number
C
0h
12h
24h
cell migration
D
cell invasion
E
PI
Annexin V-FITC
Apoptosis cells(%)

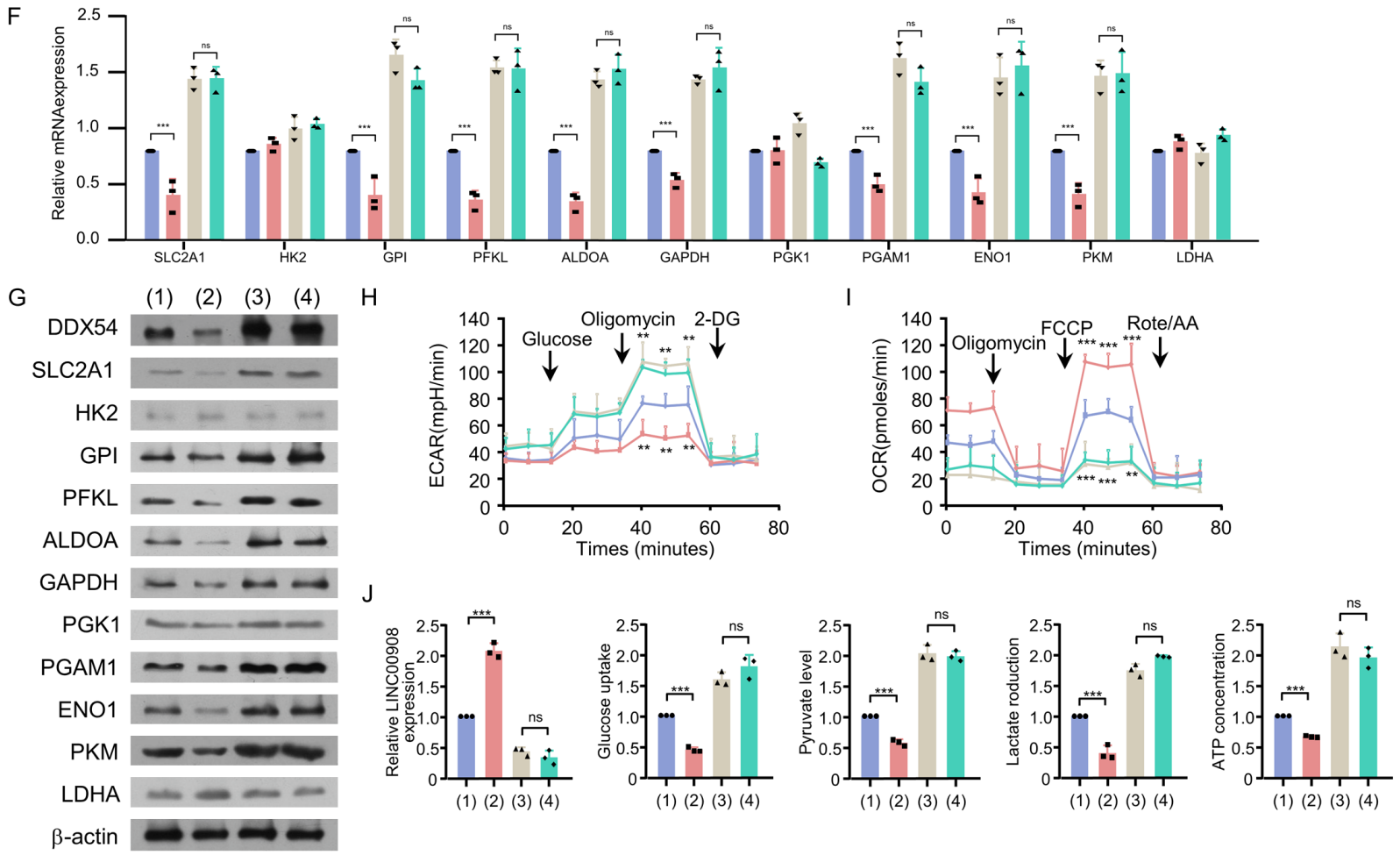

Supplementary Figure 6. RFX2 mediates proliferation, apoptosis, migration, invasion and glycolysis by regulating LINC00908 in H1299 cells. (A) A549 cells were transfected with empty vector plus scramble (1) or RFX2 plus scramble (2) or empty vector plus LINC00908 siRNAs (3) or RFX2 plus LINC00908 siRNAs (4). The immunoblot shows RFX2 in the 4 groups. LINC00908 knockdown lead to RFX2 inactivation in regulating cell proliferation. (B-E) Colony-formation, cell migration, invasion, and apoptosis of H1299 cells transfected as in (A). Histograms show proliferation, colony number, comparative cell migration and invasion, and percentage of apoptosis cells. (F and G) H1299 cells were transfected with empty vector plus scramble (1) or RFX2 plus scramble (2) or empty vector plus LINC00908 siRNAs (3) or RFX2 plus LINC00908 siRNAs (4). The mRNA and protein levels of 11 glycolysis-related genes were measured. (H-J) ECAR, OCR, Glucose uptake, Pyruvate, Lactate production and ATP production were detected. Scale bar = 50 μm. *P < 0.05, **P < 0.001, ***P < 0.0001.